Master's thesis

NTNU
Norwegian University of Science and Technology
Faculty of Natural Sciences
Department of Biotechnology and Food Science

Daniel Korneliussen

Bacillus methanolicus MGA3 as host for methanol-based production of L-tryptophan-derived specialty compounds violacein, indole and tryptamine

Master's thesis in Chemical Engineering and Biotechnology
Supervisor: Marina Gil López
Co-supervisor: Luciana Fernandes de Brito and Trygve Brautaset
July 2022

NTNU
Norwegian University of
Science and Technology

Daniel Korneliussen

Bacillus methanolicus MGA3 as host for methanol-based production of L-tryptophan-derived specialty compounds violacein, indole and tryptamine

Master's thesis in Chemical Engineering and Biotechnology
Supervisor: Marina Gil López
Co-supervisor: Luciana Fernandes de Brito and Trygve Brautaset
July 2022

Norwegian University of Science and Technology
Faculty of Natural Sciences
Department of Biotechnology and Food Science

NTNU
Norwegian University of
Science and Technology

ABSTRACT

Interest in utilising one-carbon compounds such as methanol as fuel for metabolically engineered organisms and their production of biotechnologically relevant compounds has increased in recent years. Methanol is an easily accessible compound readily assimilated by a group of bacterial species known as methylotrophs, and these serve as promising candidates to rival the more common industrial production methods that rely on sugar-based feedstocks. *Bacillus methanolicus* MGA3 is a well characterised methylotroph in which a number of value-added compounds have already been successfully produced. This study aims to explore the potential of *B. methanolicus* MGA3 as a production host for tryptophan-derived specialty compounds violacein, indole and tryptamine. Violacein is a purple pigment with interesting antibiotic properties synthesised by the *vioABCDE* operon, found naturally in species like *Chromobacterium violaceum*. Indole and tryptamine are signalling molecules involved in many biological processes and have seen usage in pharmaceuticals. Expression systems based on both theta- and rolling circle replicating plasmids with varying copy number were constructed in this study and transformed in *B. methanolicus* MGA3 with varying success. No production of violacein could be observed after attempting different cloning strategies with the violacein biosynthetic operon, likely due to the thermophilic temperature required by the production host as opposed to the psychrophilic temperature in which natural producers display violacein production. Indicators of indole production were observed via cloning of the *Escherichia coli*-derived *tnaA* gene encoding tryptophanase. Heterologous expression of the *Pseuodomonas putidas*-derived putative decarboxylase encoding gene PP_2552 for tryptamine synthesis requires further work as the project currently remains in the cloning stages. The overall results of this study provide great knowledge for future projects, recombinant bacterial strains and expression systems constructed in this study can be further explored.

SAMMENDRAG

Interesse i bruk av en-karbon forbindelser, som metanol, som energikilde for produksjon av bioteknologiske relevante stoffer har økt de siste årene. Metanol er en lett tilgjengelig forbindelse som assimileres av en gruppe bakterielle arter kalt metylotrofer, og disse artene er lovende kandidater til å utfordre de mer vanlige industrielle produksjonsmetodene som avhenger av sukkerbaserte råstoff. *Bacillus methanolicus* MGA3 er en godt studert og karakterisert metylotrof som allerede har vist seg som en produksjonsvert for en rekke verdifulle stoffer. Denne studien har som mål å utforske potensialet til *B. methanolicus* MGA3 som produksjonsvert for tryptofan deriverte spesialstoffer violacein, indol og tryptamin. Violacein er et lilla pigment med interessante antibiotiske egenskaper syntetisert av *vioABCDE* operonet, naturlig funnet i blant annet *Chromobacterium violaceum*. Indol og tryptamin er signalstoffer involvert i flere biologiske prosesser og har blitt brukt i legemidler. Uttrykkssystemer basert på theta- og ”rolling circle” replikerende plasmider med varierende kopinummer ble konstruert i dette arbeidet og transformert i *B. methanolicus* MGA3 med varierende suksess. Ingen produksjon av violacein kunne bli observert etter forsøk på flere kloningsstrategier med det violacein biosyntetiske operonet, sannsynligvis på grunn av den termofile temperaturen som kreves av produksjonsverten i motsetning til den psykrofile temperaturen der naturlige produsenter viser violaceinproduksjon. Det ble observert indikasjoner på indolproduksjon via kloning av det *Escherichia coli*-deriverte genet *tnaA* som koder for tryptofanase. Heterologt uttrykk av det *Pseudomonas putida*-deriverte antatte dekarboksylase-kodende genet PP_2552 for syntese av tryptamin behøver videre arbeid da dette prosjektet fortsatt er i kloningfasen. Resultatene fra dette arbeidet gir stor kunnskap for fremtidige prosjekter, rekombinante bakterielle stammer og plasmider konstruert i dette arbeidet kan bli utforsket videre.

PREFACE

This thesis is the product of the master's project in the Biotechnology specialisation of the two-year M.Eng. program Chemical Engineering and Biotechnology at the Norwegian University of Science and Technology (NTNU), Faculty of Natural Sciences (NV), Department of Biotechnology and Food Science (IBT).

This thesis is an expansion of the specialisation project conducted last semester, both projects at the Cell Factories group led by professor Trygve Brautaset. I would like to express my thanks to my main supervisor, Marina Gil López, for guidance and support throughout the past year, both with planning and conducting experiments as well as assistance with writing this thesis. Further thanks goes to Luciana Fernandes de Brito for additional support, and the rest of the Cell Factories group for being an inclusive, fun group to have been a part of. The environment within the group both in and outside of the lab has made my stay here very enjoyable.

All drawn figures were created with BioRender.com. Plasmid maps were created with Benchling.com.

Lastly, none of this would have been possible without the friends I have made during all my years in Trondheim. Especially everyone I have met as a part of NTNUI who have felt like my second family and been the main reason this city has become my new home. My experiences here have surpassed expectations and Trondheim will always be a big part of me.

Daniel Korneliussen, Trondheim 2022

List of Tables

List of Figures

Abbreviations used in this work

5AVA	5-aminovalerate
ATP	Adenosine triphosphate
bp/kb/Mb	Base pair/kilobase pair/megabase pair
cAMP-CRP	Cyclic adenosine monophosphate receptor protein complex
CDRP	1-(2-carboxyphenylamino) 1-deoxyribulose 5-phosphate
Cm^R	Chloramphenicol resistance
cPCR	Colony polymerase chain reaction
Cv	*Chromobacterium violaceum*
DHAP	Dihydroxyacetone phosphate
DNA	Deoxyribonucleic acid
dNTP	Deoxyribonucleotide triphosphate
ds-DNA	Double-stranded DNA
EPB	Electroporation buffer
F6P	Fructose 6-phosphate
FAD	Flavin adenine dinucleotide
Fba	Fructose 1,6-bisphosphate aldolase
FBP	Fructose 1,6-bisphosphate
GABA	γ-aminobutyric acid
GAP	Glyceraldehyde 3-phosphate
gDNA	Genomic DNA
Gln	L-glutamine
GlpX	Sedoheptulose 1,7-biphosphatase
Glu	L-glutamate
GPCR	G-protein coupled receptor
H6P	3-hexulose 6-phosphate
HPLC	High pressure liquid chromatography
Hps	3-hexulose 6-phosphate synthase
IGP	Indole 3-glycerol phosphate
IPA	Indole 3-pyruvic acid
Kn^R	Kanamycin resistance
LB	Lysogeny Broth
Lys	L-lysine
Mdh	Methanol dehydrogenase
MeOH	Methanol
mp	Methanol dehydrogenase promoter
NAD^+	Nicotinamide adenine dinucleotide
NAD(P)H	Nicotinamide adenine dinucleotide (phosphate)
NEB®	New England Biolabs®
OD_{600}	Optical density at 600 nm
OE-PCR	Overlap extension polymerase chain reaction
PCD	Programmed cell death
PCR	Polymerase chain reaction
Pfk	Phosphofructokinase
Phi	6-phospho 3-hexuloisomerase
Phe	L-phenylalanine
PQQ	Pyrroloquinoline quinone
PRA	Phosphoribosyl anthranilate
PRPP	Phosphoribosyl pyrophosphate
R5P	Ribose 5-phosphate
RBS	Ribosome binding site
RC	Rolling circle
RD	Restriction digestion
RebD	Heme containing oxidase (rebeccamycin)
RebO	Flavin dependent L-tryptophan oxidase (rebeccamycin)
Rpe	Ribulose 5-phosphate 3-epimerase
Rpi	Ribose 5-phosphate isomerase
RPM	Revolutions per minute
Ru5P	Ribulose 5-phosphate
RuMP	Ribulose monophosphate pathway
Ser	L-serine
SOB	Super optimal broth
SOE	Splicing by overlap extension
StaD	Heme containing oxidase (staurosporine)
StaO	Flavin dependent L-tryptophan oxidase (staurosporine)
T_A	Annealing temperature
TAE	Tris-acetate-EDTA
Tkt	Transketolase
TnaA	Tryptophanase
TnaB	Tryptophan permease
TnaC	Tryptophanase operon leader peptide
Trp	L-tryptophan
TrpA	α subunit of tryptophan synthase
TrpB	β subunit of tryptophan synthase
TrpC	Indole 3-glycerol phosphate synthase
TrpD	Anthranilate phosphoribosyl transferase
TrpE	Anthranilate synthase component I
TrpF	Phosphoribosyl anthranilate isomerase
TrpG	Anthranilate synthase component II
Tyr	L-tyrosine
VioA	Flavin dependent L-tryptophan oxidase (violacein)
VioB	Heme containing oxidase (violacein)
VioC	Violacein synthase
VioD	Protoviolaceinate synthase
VioE	Protodeoxyviolaceinate synthase
xp	Xylose inducible promoter
Xu5P	Xylulose 5-phosphate
ZR	Zymo Research

1. Introduction

1. Methylotrophy and methanol as alternative carbon source

Methanol is a one-carbon (C1) alcohol commonly utilised in fuels and several home and industrial applications such as paint, plastics and textiles [1]. Additionally, methanol is receiving increasing interest due to its role as a carbon source for a range of microorganisms able to produce valuable biochemicals. Bacteria able to utilise C1 compounds as carbon and energy source are classed as methylotrophic bacteria [2]. Advantages of using C1 compounds like methanol as carbon sources over more traditional sugar compounds include their easy availability as many are either waste products of other processes or can be synthesised at relatively low costs [3, 4], as well as the avoidance of competing with the food industry which involves the rising prices of sugar-based feedstocks [5, 6].

Methanol is commonly produced from natural gas which can be reformed through a variety of approaches. The most widely used method is steam reforming, several other methods have been utilised more and more in recent times which include autothermal reforming, dry methane reforming and gas heated reforming. The result of natural gas reforming is a synthesis gas (syngas) comprised of different ratios of H_2, CO and CO_2. Syngas produces methanol by reactions of CO and CO_2 with hydrogen according to Equations 1.1 and 1.2. The water gas shift reaction (1.3) also influences the reaction mechanisms [7].

$$CO_2 + 3\,H_2 \longrightarrow H_2O + CH_3OH \tag{1.1}$$

$$CO + 2\,H_2 \longrightarrow CH_3OH \tag{1.2}$$

$$CO + H_2O \longrightarrow CO_2 + H_2 \tag{1.3}$$

These reactions are carried out industrially at high temperatures and pressures (200-300 °C and 50-100 bar) with a $Ni/Zn/Al_2O_3$ catalyst [7]. Due to the energy requirements and costs of indirect methanol production via syngas, alternative approaches are being explored which include the direct conversion of methane into methanol. However such methods have not been commercialised as of yet because of the strong C-H bond in methane which is difficult to activate as well as poor selectivity for methanol [8].

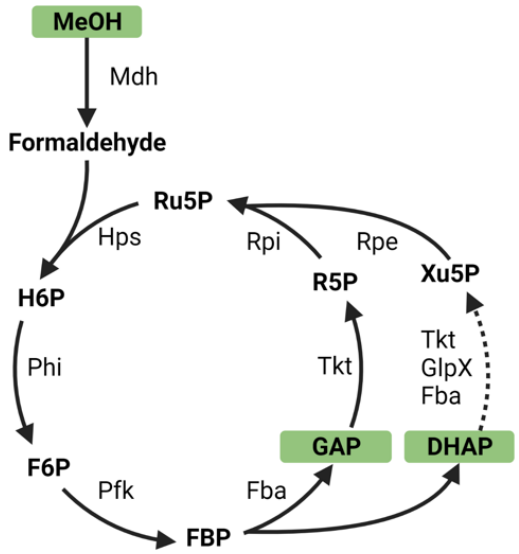

Fig. 1.1: Overview of methanol and formaldehyde assimilation in the Gram-positive methylotroph *Bacillus methanolicus* MGA3, via the RuMP cycle. Dashed lines indicate several reaction steps. Abbreviations for enzymes and metabolites can be found in the text.

Previous research exploring the potential of C1 compounds, specifically methanol, has shown that the first step of methanol assimilation in prokaryotes involve oxidation to formaldehyde by methanol dehydrogenase (Mdh), using pyrroloquinoline quinone (PQQ) or nicotinamide adenine dinucleotide (NAD^+) as electron acceptors in Gram-negative and Gram-positive bacteria, respectively [9]. Formaldehyde is a cytotoxic compound with a high level of nonspecific reactivity with proteins and nucleic acids. All living organisms have had to acquire pathways for formaldehyde assimilation, dissimilation or detoxification in order to survive, as small amounts of formaldehyde are produced by demethylation reactions in all organisms [9]. The toxicity of formaldehyde arises from formation of reactive dihydroxymethyl peroxides and free radicals which cause oxidative stress and cell death [10, 11]. In bacteria, formaldehyde is assimilated quickly after formation through either the ribulose monophosphate pathway (RuMP) or the serine (Ser) pathway [12].

Formaldehyde assimilation via the RuMP cycle involves two enzymes which, along with Mdh, are specific for methylotrophic bacteria; 3-hexulose 6-phosphate synthase (Hps) and 6-phospho 3-hexuloisomerase (Phi). Ribulose 5-phosphate (Ru5P) reacts with formaldehyde through the actions of Hps to form hexulose 6-phosphate (H6P) which is further converted to fructose 6-phosphate (F6P) by Phi. The remaining steps of the RuMP cycle are catalysed by enzymes not specific to methylotrophy, starting with phosphofructokinase (Pfk) which converts F6P to fructose 1,6-bisphosphate (FBP). FBP is then cleaved by fructose 1,6-bisphosphate aldolase (Fba) to produce the key metabolites glyceraldehyde 3-phosphate (GAP) and dihydroxyacetone phosphate (DHAP) which are central intermediates in many metabolic pathways, for instance glycolysis [13]. They can also continue the RuMP cycle where DHAP is converted in several steps to xylulose 5-phosphate (Xu5P) by Fba, transketolase (Tkt) and sedoheptulose 1,7-biphosphatase (GlpX) and further to Ru5P by ribulose 5-phosphate 3-epimerase (Rpe), while GAP can be converted to ribose 5-phosphate (R5P) by Tkt and back to Ru5P by ribose 5-phosphate isomerase (Rpi) [14, 15]. The organism of interest for this study is *Bacillus*

methanolicus MGA3 which utilises the RuMP cycle for carbon uptake. An overview of the methanol assimilation in *B. methanolicus* MGA3 is illustrated in Figure 1.1 [13]. Additionally, *B. methanolicus* is able to oxidise formaldehyde to CO_2 in both cyclic and linear dissimilatory pathways [14, 16].

2. B. methanolicus MGA3 as a production host

B. methanolicus is a well studied methylotrophic bacterium; it is a Gram-positive, thermophilic, facultative methylotroph that uses the RuMP cycle for formaldehyde assimilation. *B. methanolicus* is readily isolated from wastewater and soil samples, growing optimally at 50-53 °C [14, 17]. The wild type strain MGA3 is the most characterised strain of *B. methanolicus*, having been fully sequenced in 2014, revealing a 3 Mb circular chromosome as well as the two natural plasmids pBM19 and pBM69 [18]. Methanol assimilation in *B. methanolicus* MGA3 depends on genes both on the chromosomal DNA and pBM19 to manage the RuMP cycle [18]. For instance, one of the *mdh* gene copies is carried by pBM19 together with five other central RuMP genes; *pfk*, *fba*, *tkt*, *glpX* and *rpe*, all of which continue the RuMP cycle after formation of F6P (Figure 1.1) [19]. The *hps* and *phi* genes in *B. methanolicus* MGA3 are located on the chromosome and are induced by formaldehyde rather than methanol [19]. These genes are critical for methanol assimilation and it has been shown that introducing multiple copies of *hps* and *phi* to wild type MGA3 increases the assimilation rates as well as the methanol tolerance of the cell [19]. The fact that these genes are chromosomal and specific for methylotrophic bacteria means that transfer of the *mdh*-carrying pBM19 plasmid alone to non-methylotrophic bacteria would be lethal when methanol is present in the environment, due to formation of toxic formaldehyde without a way to initiate the RuMP cycle [19, 20].

B. methanolicus MGA3 has already been used for production of several valuable compounds from methanol. Brautaset *et al*. reported yields of 58 g/L and 37 g/L of the amino acids glutamine (Gln) and lysine (Lys), respectively [14]. Cadaverine yields of 10.2 g/L and 11.3 g/L have been reported in *B. methanolicus* MGA3 [21, 22], as well as 9 g/L γ-aminobutyric acid (GABA) [23], all in fed-batch fermentations. Further studies report yields of 0.42 g/L acetoin [24] and 0.02 g/L 5-aminovalerate (5AVA) [25] in shake-flask cultivations. These reports demonstrate the applicability of *B. methanolicus* MGA3 as a production host. Being a well characterised organism, several tools for genetic engineering of *B. methanolicus* MGA3 have been developed [21], several of which form the basis of the work conducted in this study. Additional tools for gene knockouts have been developed for *B. methanolicus* MGA3 by use of CRISPR interference [26].

Due to its thermotolerant nature, *B. methanolicus* MGA3 is a suitable candidate host for industrial applications as the demands for cooling are lower compared to alternative hosts growing at mesophilic temperatures, this temperature also decreases the chances of contamination. However, a drawback of these conditions is the decreased solubility of oxygen, requiring extra attention to the oxygen supply [14], as well as being an obstacle for production of some compounds [27].

3. Trytophan and tryptophan-derived compounds

L-tryptophan (Trp) is an essential amino acid which humans are unable to synthesise, dietary uptake being the only source of Trp in humans. Trp is the least abundant of all 20 proteinogenic amino acids [28], it is commonly acquired through breakdown of proteins from fruits, dairy products, bread and meats [29]. The many roles of Trp include involvement in protein synthesis and being a precursor to the signalling molecules serotonin and melatonin, among others [29, 30]. Trp depletion has been reported to affect mood, cognitive processes and behaviour [29]. Trp is a component of several therapeutics such as antidepressants and treatment of seasonal affective disorder and sleep disorders [29]. Trp is a precursor to many different products and intermediates as shown in Figure 1.2. The focus of this study is on the Trp derivatives violacein, indole and tryptamine which will be discussed in more detail.

Trp biosynthesis occurs in a range of different bacterial species via the *trp* operon, consisting of seven genes (*trpABCDEFG*) [31]. Regulation of the *trp* operon is accomplished by many different mechanisms depending on the organism and the order of the genes within the operon also differs greatly among Trp producing organisms [31]. The genes can even be located in different operons, as is the case in *Bacillus subtilis* where *trpG* is located in the folate operon [32]. The initial precursor of Trp is chorismate, this is also the branch-point for synthesis of the other aromatic amino acids tyrosine (Tyr) and phenylalanine (Phe) [33]. Chorismate is itself synthesised via the shikimate pathway [34]. In Trp biosynthesis, chorismate and Gln are converted to anthranilate by anthranilate synthase which is a polypeptide complex encoded for by *trpE* and *trpG* [35]. Encoded for by *trpD* is anthranilate phosphoribosyl transferase which converts anthranilate and phosphoribosyl pyrophosphate (PRPP) to phosphoribosyl anthranilate (PRA) [36]. Enzymes encoded for by *trpF* (PRA isomerase) and *trpC* (IGP synthase) catalyse the next steps, converting PRA to indole 3-glycerol phosphate (IGP) via 1-(2-carboxyphenylamino) 1-deoxyribulose 5-phosphate (CDRP) [37]. Trp synthase consists of an α and β subunit encoded for by *trpA* and *trpB*, respectively. TrpA converts IGP to indole, which further combines with Ser in a reaction catalysed by TrpB to form Trp [38]. Some prokaryotes have two variants of *trpB*, one of which encodes for the β subunit of Trp synthase while the other is suspected to encode for an enzyme acting as a Ser deaminase [39, 40]. Many bacteria have been metabolically engineered for overproducing Trp, these include *Corynebacterium glutamicum* engineered to produce approximately 50 g/L Trp [41, 42], and *E. coli* with reported titers of up to 50 g/L Trp, both in fed-batch fermentations [41, 43, 44]. Current work is also assessing *B. methanolicus* as a production host for Trp with a current titer of 0.2 g/L in shake flask cultivations [45].

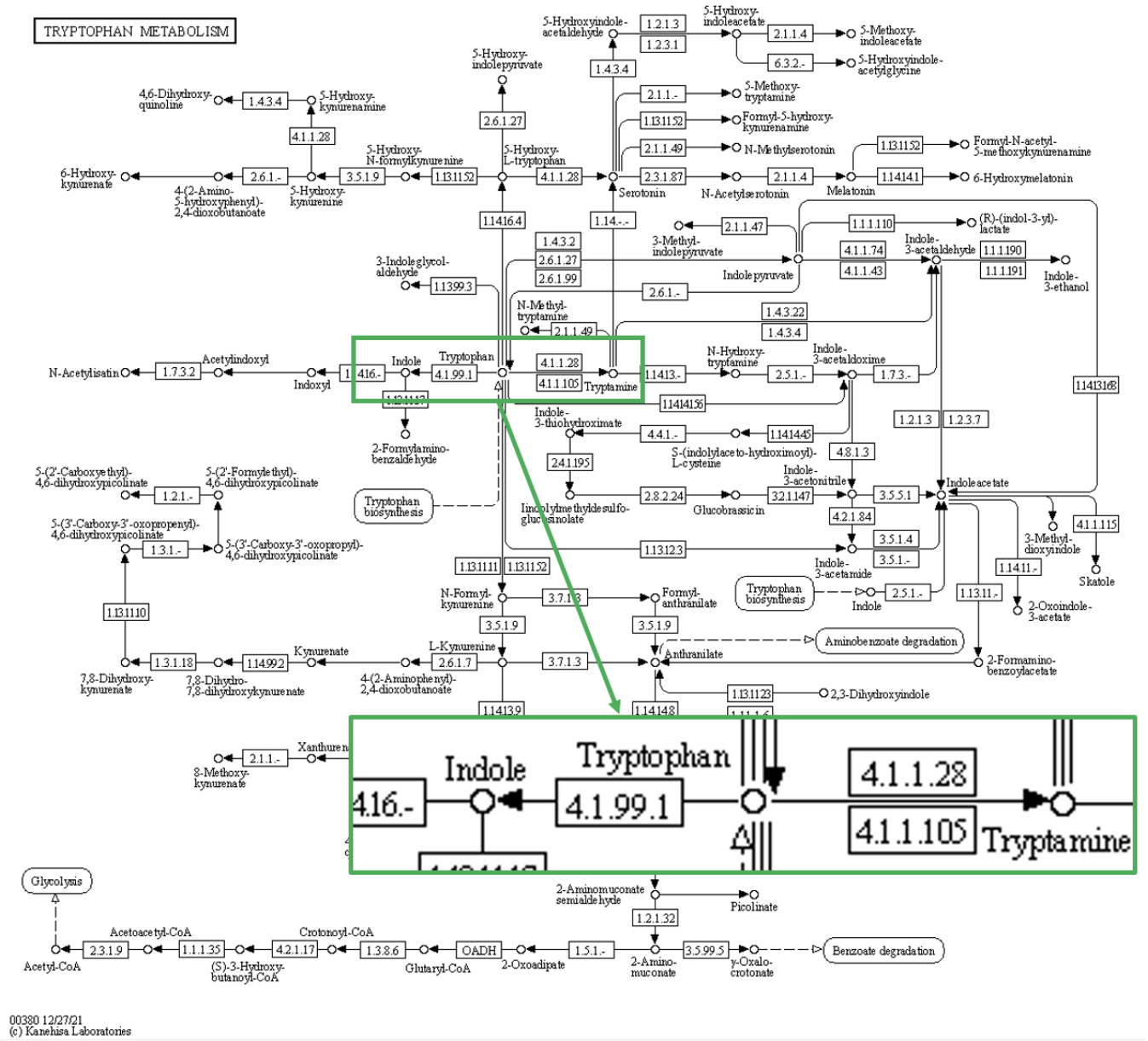

Fig. 1.2: Pathway map of L-tryptophan metabolism retrieved from the Kegg database. Selected pathways are highlighted; indole and tryptamine synthesis pathways, produced from L-tryptophan by the action of tryptophanase and a tryptophan decarboxylase, respectively. Violacein is not shown.

1) Violacein: The molecular structure of violacein is shown in Figure 1.3, violacein can be divided into three parts; 5-hydroxyindole, oxindole and 2-pyrrolidone [46]. Violacein is a purple pigment, the biological activities of which have been explored in previous studies. These include antioxidant, antimicrobial and immunomodulatory activities [47]. Its most interesting property is its antitumour potential: violacein has been reported to induce programmed cell death (PCD) in normally resistant TF1 leukemia cells [47] and more recent studies have further explored its potential in other cell lines, including glioblastoma (U87), breast cancer (MCF7) and lung cancer (A549) [6, 48].

Violacein synthesis depends on a series of reactions catalysed by five separate enzymes encoded for by the *vioABCDE* gene cluster, which is found naturally in *Chromobacterium violaceum*,

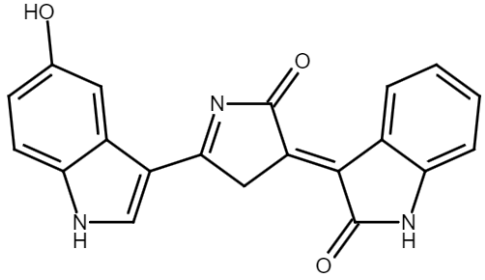

Fig. 1.3: Molecular structure of violacein. It consists of 5-hydroxyindole (left) and oxindole (right) connected by 2-pyrrolidone.

Janthinobacterium lividum and *Duganella* sp. B2, among others [49]. Violacein is synthesised from Trp, with the synthesis pathway illustrated in Figure 1.4. The first enzyme, a flavin-dependent Trp 2-monooxygenase encoded for by *vioA*, oxidises one Trp to indole 3-pyruvic acid (IPA) imine, aided by co-factor FAD, which constitutes the oxindole part of the violacein molecule. Next, a heme containing oxidase encoded for by *vioB* catalyses the formation of an IPA imine dimer by combining the oxindole with another molecule of Trp whose amino-group forms the middle structure of violacein - 2-pyrrolidone (Figure 1.4a). This dimer is short-lived and is quickly rearranged in a 1-2 shift by a protodeoxyviolaceinate synthase encoded for by *vioE* to produce protodeoxyviolaceinic acid. This is subsequently hydroxylated by a protoviolaceinate synthase (*vioD*) to form protoviolaceinic acid. Further oxidation by violacein synthase (*vioC*) produces violaceinic acid which undergoes a spontaneous, non-enzymatic reaction to produce violacein (Figure 1.4b). In the absence of VioD, deoxyviolaceinic acid is produced which is further converted to deoxyviolacein. An impure mixture of violacein and deoxyviolacein is the most common product of violacein synthesis, called crude violacein. The absence of VioC results in the formation of proviolacein (or prodeoxyviolacein in the absence of both VioC and VioD) [6, 46, 50, 51, 52, 53].

Additional products can be synthesised from the IPA imine dimer; rebeccamycin and staurosporine whose synthesis pathways coincide with the first stages of violacein synthesis. The enzymes RebO and StaO are Trp 2-monooxygenases which perform the same role as VioA by converting Trp to IPA imine, likewise, RebD and StaD converts this further to the IPA imine dimer by oxidation in the same reaction as catalysed by VioB. A spontaneous reaction converts the dimer to chromopyrrolic acid which can undergo a series of enzymatic reactions to produce either rebeccamycin or staurosporine. VioE is therefore a critical enzyme in violacein synthesis to avoid formation of chromopyrrolic acid [49].

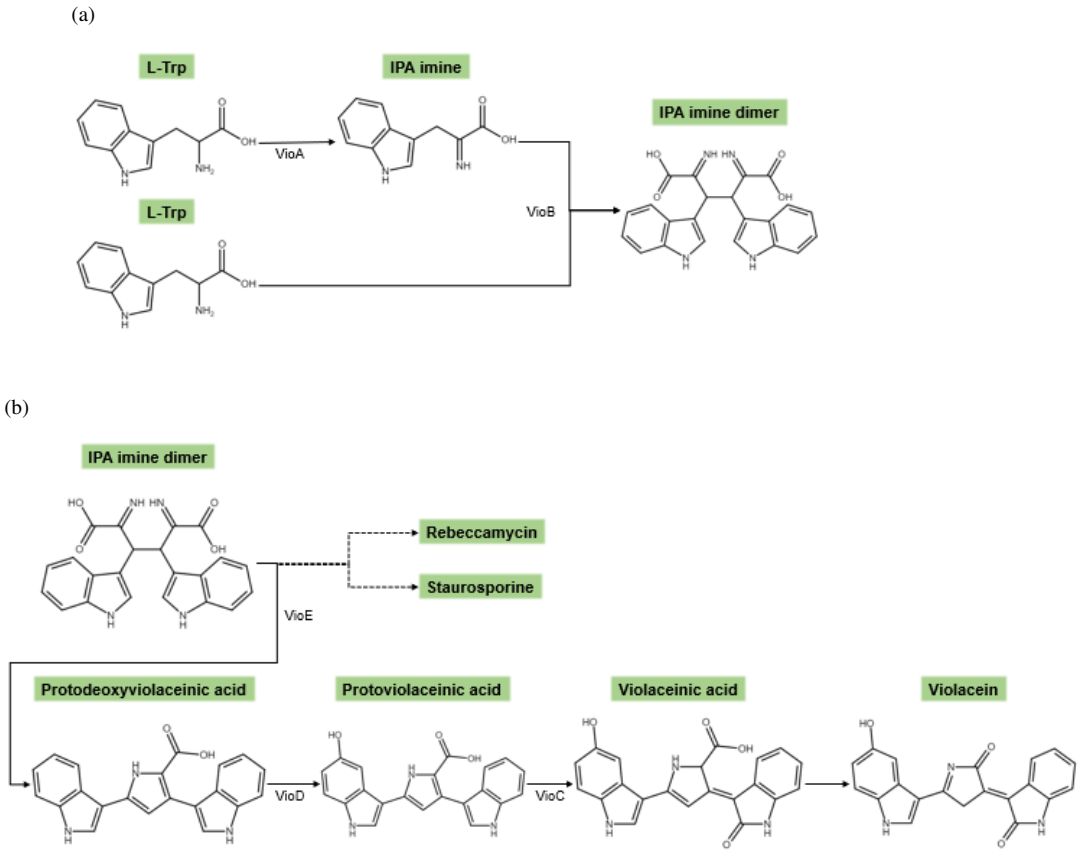

Fig. 1.4: (a) Synthesis of the IPA imine dimer in the violacein synthesis pathway. VioA oxidises Trp to IPA imine, which is combined with another molecule of Trp to form an IPA imine dimer, in a reaction catalysed by VioB. (b) Synthesis pathway of violacein. An IPA imine dimer is converted into protodeoxyviolaceinic acid by vioE. Further hydroxylation and oxidation by VioD and VioC, respectively, produces protoviolaceinic acid and violaceinic acid, the latter of which undergoes a spontaneous, non-enzymatic reaction to form violacein. VioC catalyses the formation of deoxyviolaceinic acid as well which is converted to deoxyviolacein, crude violacein consists of both violacein and deoxyviolacein. IPA imine dimer is also a precursor for rebeccamycin and staurosporine.

2) Indole: Indole (Figure 1.5) is primarily a signalling molecule that regulates physiological processes in a range of host bacteria and is produced naturally by over 85 Gram-positive and Gram-negative bacteria [54]. As a signalling molecule, indole regulates processes such as motility, biofilm formation and antibiotic resistance. Furthermore, indole can extend its effects such as antibiotic resistance to non-indole producing species. Indole also functions in mammals by balancing inflammation in the intestinal tract [54, 55]. Indole is commonly produced by *E. coli* in the gastrointestinal tract [56], with indole synthesis in *E. coli* K-12 substr. MG1655 having been well studied and documented [57]. Indole in *E. coli* is synthesised from Trp by action of a tryptophanase (TnaA) in a reaction that also produces pyruvate and ammonia as shown in Equation 1.4 [55].

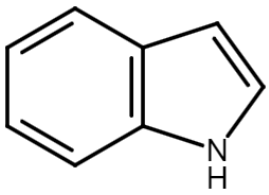

Fig. 1.5: Molecular structure of indole, composed of a benzene ring fused with a pyrrole ring.

$$\mathrm{Trp} + \mathrm{H_2O} \xrightarrow{\mathrm{TnaA}} \mathrm{Indole} + \mathrm{C_3H_4O_3} + \mathrm{NH_3} \tag{1.4}$$

The *tnaA* gene is located in the *tnaCAB* operon. Transcription of *tnaAB* is activated by the cAMP-CRP complex and induced by Trp, with a Rho-dependent terminator and a TnaC leader peptide. TnaB is a transporter that imports Trp, with high concentrations of Trp being required for induction of *tnaA* transcription [55].

3) Tryptamine: Tryptamine (Figure 1.6) is a neurotransmitter synthesised via decarboxylation of Trp by aromatic amino acid decarboxylases. PP_2552, found in *Pseudomonas putida* KT2440, is annotated in its genome as coding for one such decarboxylase, more precisely a putative Trp decarboxylase [58]. Tryptamine is commonly produced by gut bacteria where its effects include increasing fluid secretion in the colon via the G-protein coupled receptor (GPCR) 5-HT_4R [58, 59]. Tryptamine is also a natural precursor to other compounds such as serotonin, an important signalling molecule, and multiple hallucinogenic and toxic substances as well as anti-migraine drugs [60]. The effects of tryptamine on several animal species, such as mouse, rat and guinea pig, include weak behavioural excitation, an effect that is enhanced by inhibition of monoamine oxidases [61].

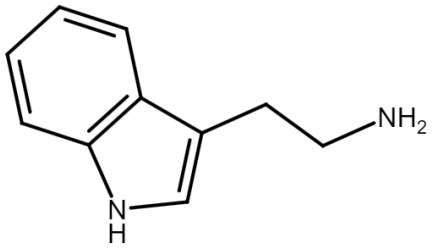

Fig. 1.6: Molecular structure of tryptamine, composed of indole and a 2-aminoethyl group.

4. Aim of this study

The aim of the study is to create recombinant strains of *B. methanolicus* MGA3 for production of the selected Trp-derived compounds violacein, indole and tryptamine, as well as to further expand the scope of this organism as a production host. Expression systems containing *vioABCDE* will be constructed for *B. methanolicus* MGA3 using the genetic donor *C. violaceum*. Different combinations of the *vio* genes will be inserted into different expression systems in order to control expression of individual genes for optimal violacein production. Bottlenecks in the violacein synthesis pathway and other similar problems will be explored using the different expression systems. As an example, VioC oxidises both protodeoxyviolaceinic acid and protoviolaceinic acid which leads to synthesis of a non-pure final product containing both deoxyviolacein and violacein. Therefore, one of the strategies envisioned in this work is the overexpression of VioD making use of a high copy number plasmid to increase the hydroxylation rate of protodeoxyviolacein [6]. The effects of optimised ribosome binding sites (RBS) on violacein production will also be explored in this study.

Expression systems for production of indole will be constructed using *E. coli* K-12 as genetic donor for *tnaA*. Note that indole is a precursor in biosynthesis of Trp, where TrpB as the β subunit of Trp synthase is responsible for catalysing the conversion of indole to Trp [38]. The reverse reaction, conversion of Trp to indole, is catalysed by TnaA according to Equation 1.4, this reaction also produces pyruvate and ammonia [55]. Under certain conditions, this reaction has shown to be reversible, although the rate of the reverse reaction is fairly low ($<$2 nmol/min). Furthermore, pyruvate and ammonia are consumed by other metabolic pathways, preventing buildup of these compounds which would otherwise push the reaction back towards Trp formation [62]. The strategy for indole production involves overexpressing *tnaA* to accumulate indole, deeming the effects of the reverse reaction negligible.

Tryptamine is synthesised from Trp by the putative decarboxylase PP_2552 from *P. putida* KT2440 in a straightforward reaction [58]. As Trp is the direct precursor for tryptamine and only one gene being involved in the tryptamine biosynthesis, overexpression of PP_2552 is therefore the strategy for tryptamine production.

The *vioABCDE* expression systems are based on the pNW33Nmp and pBV2xp vectors [21]. The former is a rolling circle (RC) replicating plasmid under control of the *mdh* promoter (mp) while the latter is a theta-replicating plasmid based on pHCM04 under control of a xylose inducible promoter (xp) [21]. The pNW33Nmp vector is one of the earliest expression vectors used for overexpression of genes in *B. methanolicus* MGA3, however despite having a higher copy number, later studies have reported higher gene expression using vectors containing the pHCM04 replicon, likely due to higher replicon

stability [6, 21, 63]. Another RC replicating plasmid, based on pUB110 - pUB110Sxp, under control of the xp promoter - will also be used as expression vector for the *tnaA* and PP_2552 genes, this is reported to be a high copy number plasmid [21].

Finally, all recombinant *B. methanolicus* MGA3 strains will use the Trp overproducer Trp3 constructed in a separate study [45] to fuel the production of the Trp derivatives violacein, indole and tryptamine.

2. Materials and Methods

1. Bacterial strains and cultivation conditions

Bacterial strains and plasmids used in this study are listed in Table 2.1, 2.2 and 2.3. *Escherichia coli* DH5α was used as general cloning host, *E. coli* S17-1 was used as donor strain for conjugation and *B. methanolicus* MGA3 was used as expression host. *C. violaceum* MK, *E. coli* K-12 and *P. putida* KT2440 were used as source organisms for *vioABCDE*, *tnaA* and PP_2552, respectively.

Table 2.1: List of bacterial strains used in this study

Strain name	Description	Ref.
E. coli DH5α	General cloning host, F-*thi*-1 *endA*1 *hsdR*17(r-,m-) *supE*44 _*lacU*169 (_80*lacZ*_M15) *recA*1 *gyrA*96 *relA*1	[64]
E. coli S17-1	Donor strain for conjugation, *recA*, *thi*, *pro*, *hsd* R-M+	ATCC 47055
E. coli K-12	Wild type strain, source organism for *tnaA*	DSM 18039
C. violaceum MK	Wild type strain, source organism for *vioABCDE*	DSM 30191
P. putida KT2440	Wild type strain, source organism for PP_2552	DSM 6125
B. methanolicus MGA3	Wild type strain, expression host	ATCC 53907

Table 2.2: List of plasmids used and constructed in this study

Plasmid name	Description	Ref.
pBV2xp	Kn^R; pBV2 derivative for gene expression under control of the xp promoter	[24]
pBV2xp-$pVio^{Cv}$	Kn^R; pBV2xp derivative for expression of *vioABCDE* from *C. violaceum* under control of the xp promoter	[65]
pBV2xp-*vioACD*	Kn^R; pBV2xp derivative for *vioACD* expression under control of the xp promoter	This study
pNW33Nmp	Cm^R; pNW33N derivative for gene expression under control of the mp promoter	[21]
pNW33Nmp-*vioBE*	Cm^R; pNW33Nmp derivative for *vioBE* expression under control of the mp promoter	This study
pNW33Nmp-*vioD*	Cm^R; pNW33Nmp derivative for *vioD* expression under control of the mp promoter	This study
pNW33Nmp-*vioE*	Cm^R; pNW33Nmp derivative for *vioE* expression under control of the mp promoter	This study
pUB110Sxp	Kn^R; pUB110S derivative for gene expression under control of the xp promoter	[21]
pUB110Sxp-*tnaA*	Kn^R; pUB110Sxp derivative for *tnaA* expression under control of the xp promoter	This study
pTH1mp-Trp3	Cm^R; pTH1mp derivative for *trpDGE* expression under control of the mp promoter	[45]

Kn^R: kanamycin resistant.
Cm^R: chloramphenicol resistant.
xp: xylose inducible promoter.
mp: methanol dehydrogenase promoter.

Table 2.3: List of recombinant bacterial strains constructed in this study

Strain name	Ref.
B. methanolicus MGA3(pBV2xp)	This study
B. methanolicus MGA3(pNW33Nmp)	This study
B. methanolicus MGA3(pUB110Sxp)	This study
B. methanolicus MGA3(pBV2xp-*vioACD*)	This study
B. methanolicus MGA3(pNW33Nmp-*vioBE*)	This study
B. methanolicus MGA3(pNW33Nmp-*vioD*)	This study
B. methanolicus MGA3(pNW33Nmp-*vioE*)	This study
B. methanolicus MGA3(pBV2xp-*vioACD*)(pNW33Nmp-*vioBE*)	This study
B. methanolicus MGA3(pTH1mp-Trp3)(pUB110Sxp-*tnaA*)	This study
E. coli DH5α(pBV2xp-*vioACD*)	This study
E. coli DH5α(pNW33Nmp-*vioBE*)	This study
E. coli DH5α(pNW33Nmp-*vioD*)	This study
E. coli DH5α(pNW33Nmp-*vioE*)	This study
E. coli S17-1(pBV2xp-*vioABCDE*)	This study
E. coli S17-1(pBV2xp-*vioACD*)	This study
E. coli S17-1(pNW33Nmp-*vioBE*)	This study
E. coli S17-1(pNW33Nmp-*vioD*)	This study
E. coli S17-1(pNW33Nmp-*vioE*)	This study

Composition of growth media can be found in Appendix B. All *E. coli* strains were cultivated at 37°C and 275 RPM in Lysogeny Broth (LB) media or on LB agar plates, both supplemented with antibiotics; 50 µg/mL kanamycin or 15 µg/mL chloramphenicol when appropriate. *B. methanolicus* MGA3 main cultures were cultivated at 50°C and then transferred to 30 or 37°C, always at 200 RPM, in SOB or MVcM media supplemented with antibiotics; 25 µg/mL kanamycin or 5 µg/mL chloramphenicol when appropriate. *B. methanolicus* MGA3 pre-cultures were cultivated at 50°C and 200 RPM in SOB or MVcMY media supplemented with antibiotics; 25 µg/mL kanamycin or 5 µg/mL chloramphenicol when appropriate. *B. methanolicus* MGA3 strains were also cultivated on SOB agar plates supplemented with antibiotics; 25 µg/mL kanamycin or 5 µg/mL chloramphenicol when appropriate. Glycerol stocks were prepared by adding 650 µL bacterial culture to 350 µL 89% glycerol and stored at -80°C.

2. Molecular cloning and DNA work

1) Isolation of genomic and plasmid DNA:
Genomic DNA (gDNA) was isolated from source organisms in order to acquire template DNA for PCR. Source bacteria were cultivated overnight and harvested the next day by centrifugation at 3000 RPM and 25°C for one minute. Isolation of gDNA was performed using the Monarch® Genomic DNA Purification Kit (New England Biolabs, NEB), following the manufacturer's protocol. Isolation of plasmid DNA from general cloning hosts was performed using the ZR Plasmid Miniprep™ - Classic Kit (Zymo Research, ZR), following the manufacturer's protocol, in order to acquire plasmids for further molecular cloning and transformations. *E. coli* DH5α harbouring plasmid of interest was cultivated overnight and harvested by centrifugation at 7830 RPM and 25°C for five minutes. Concentration of isolated gDNA and plasmid DNA was measured on NanoDrop™ One (Thermo Scientific™).

2) Plasmid restriction:
Restriction digestion (RD) was performed on plasmids for preparation of vector construction. RD was performed using NEB® buffers and restriction enzymes. Ten µL of appropriate buffer was mixed with 2 µL chosen restriction enzyme(s) and 2 µg plasmid DNA, the mixture was filled to 100 µL with MilliQ H_2O and incubated at 37°C for one hour.

3) Vector dephosphorylation:
FastAP Thermosensitive Alkaline Phosphatase (Thermo Scientific™) was used to dephosphorylate cloning vectors in order to avoid recircularisation of the empty vector during ligation. Four µL FastAP buffer was mixed with 2 µL FastAP Thermosensitive Alkaline Phosphatase and up to 2 µg cut plasmid DNA in a total of 40 µL MilliQ H_2O. The mixture was incubated at 37°C for 15 minutes followed by DNA purification using the QIAquick PCR Purification kit (Qiagen), following the manufacturer's protocol, and the concentration was measured on NanoDrop™ One (Thermo Scientific™).

4) Polymerase chain reaction for DNA amplification:
All DNA primers used in this study are found in Table A.1. Polymerase chain reaction (PCR) was used to amplify DNA fragments *in vitro*, this method consists of three steps: denaturation where the ds-DNA is separated into two strands; annealing where primers bind to complementary sequences in the denatured DNA, each pair of primers has its own annealing temperature (T_A) for optimal binding; and finally extension of the DNA strands by DNA polymerase. PCR was performed using CloneAmp™ HiFi PCR Premix Protocol-At-A-Glance (Takara), following the manufacturer's protocol, in a C1000 Touch Thermal cycler (Bio-Rad) or Mastercycler Nexus 32 (Eppendorf). The PCR program is described in Table 2.4. The CloneAmp™ reaction mixture consists of 12.5 µL CloneAmp™ HiFi PCR Premix, 0.5 µL forward primer, 0.5 µL reverse primer, 1.0 µL template DNA at a concentration of $<$100 ng/µL and 10.5 µL MilliQ H_2O. DNA fragments were confirmed by agarose gel electrophoresis.

Table 2.4: General PCR program

Temp. (°C)	Time (s)	Purpose	Cycles
98	10	Denaturation	1
T_a (Table A.1)	15	Annealing	35
72	5 /kb	Extension	1

Overlap extension PCR (OE-PCR) is an alternative cloning method which does not require restriction enzymes, this method can be utilised to splice DNA fragments together in a process called gene splicing by overlap extension, or "gene SOEing". Special primers are developed that create overhangs at the ends of the first DNA fragment which are complementary to the ends of the second DNA fragment, and likewise primers for the second fragment. This mixture is denatured in order to separate all the DNA strands. Some of the original ds-DNA fragments will be reformed by re-annealing, but the complementary overhang regions of the different fragments can also anneal to each other, and in the extension step the DNA polymerase will extend these regions in the 3'-direction of both fragments until it runs out of template. The end result is a mixture of the original ds-DNA fragments as well as longer fragments in which both ds-DNA molecules have been

combined. Finally, purification PCR is performed using only the end primers of the desired product in order to amplify this fragment [66, 67].

Primers used for OE-PCR are found in Table A.2 and fragments to be spliced were initially amplified following the protocol in Table 2.4. The fragments were purified using the QIAquick PCR Purification Kit (Qiagen), following the manufacturer's protocol, and the concentrations were measured on NanoDrop™ One (Thermo Scientific™). Equimolar amounts of purified fragments were mixed in 12.5 µL CloneAmp™ HiFi PCR Premix (Takara). Fifteen cycles of a two-step PCR program were run with this mixture and upon completion of the program, end primers of the desired product were added and another 20 cycles of the two-step PCR program were run. The two-step PCR program is given in Table 2.5. DNA fragments were confirmed by agarose gel electrophoresis.

Table 2.5: Overlap extension PCR program

Temp. (°C)	Time (s)	Purpose
98	10	Denaturation
68	30-60 /kb	Extension

5) Agarose gel electrophoresis:
Amplified DNA fragments were separated and visualised on gels consisting of 0.8% (w/v) agarose in Tris-acetate-EDTA (TAE) buffer supplemented with 20 µL GelRed. Separation and visualisation were performed with electrophoresis. DNA Gel Loading Dye 6X (Thermo Scientific™) was applied to samples and loaded into the wells, GeneRuler 1 kb Plus DNA Ladder (Thermo Scientific™) or 1 kb Plus DNA Ladder (NEB) was used as marker. The gel electrophoresis was run for 30-40 minutes at 100 V and 400 A in TAE buffer, the finished gel was visualised in UV-light by ChemiDoc XRS+ Gel Imaging System (Bio-Rad).

6) Vector construction:
DNA fragments from PCR and restricted cloning vectors were purified using the QIAquick PCR Purification Kit (Qiagen), following the manufacturer's protocol, and the concentrations were measured on NanoDrop™ One (Thermo Scientific™). Assembly of linearised plasmids and amplified DNA fragments for construction of expression vectors was performed using the Gibson Assembly method [68].

7) Construction of cloning host:
E. coli DH5α was used as a general cloning host, using chemically competent DH5α cells. Transformation of *E. coli* DH5α cells was performed by the heat shock method. Chemically competent cells were thawed on ice and assembled expression vector was added to the cells, the cells were incubated on ice for 30 minutes. The cells were then exposed to 42°C for 1.5 minutes and regenerated on ice for three minutes directly afterwards. The cells were incubated in 1 mL LB media at 37°C for one hour. Recombinant DH5α cells were harvested by centrifugation at 7830 RPM for 3 minutes and plated on LB plates supplemented with appropriate antibiotics. The plates were incubated at 37°C for up to 24 hours, or until visible growth of single colonies. Colony PCR (cPCR) was performed on single colonies using GoTaq® DNA Polymerase; 2µL GoTaq® 5X Green Buffer was mixed with 0.2 µL dNTP mixture, 0.2 µL forward primer, 0.2 µL reverse primer, 0.05 µL GoTaq® DNA Polymerase in a total of 10.0 µL mixture, remaining volume was filled with MilliQ H_2O. cPCR was performed according to Table 2.6, a list of cPCR primers is found in Table A.3. Finally, positive clones were confirmed by agarose gel electrophoresis.

Table 2.6: General colony PCR program

Temp. (°C)	Time (min)	Purpose	Cycles
95	10	Initial denaturation	1
95	1	Denaturation	
T_a (Table A.1)	1	Annealing	35
72	1 /kb	Extension	
72	5 /kb	Final extension	1

8) Sequencing:
Positive clones from cPCR were incubated at 37°C for up to 24 hours in LB media supplemented with appropriate antibiotics. Plasmid DNA was isolated from the grown culture and its concentration measured on NanoDrop™ One (Thermo Scientific™). Plasmid DNA was prepared for sequencing by adding 2.5 µL primer to 7.5 µL isolated plasmid DNA (400-500 ng, diluted if necessary), sequencing primers are listed in Table A.3. Sequencing was performed by Eurofins Genomics using Sanger sequencing method. The Benchling alignment tool was used to examine the sequencing results.

3. Construction of recombinant B. methanolicus MGA3 strains

1) Preparation of electrocompetent B. methanolicus cells:

B. methanolicus MGA3 cells were prepared for electroporation using the following protocol. A pre-culture of *B. methanolicus* MGA3 was incubated to optical density at 600 nm (OD_{600}) of 2.0-2.5, 50 µL of pre-culture was incoulated in 25 mL SOB medium and incubated at 50°C and 200 RPM overnight. The culture was re-inoculated to an initial OD_{600} of 0.1-0.2 into 25 mL of SOB medium pre-warmed to 50°C and incubated at 50°C and 200 RPM for 3-4 hours. The culture was re-inoculated once more to OD_{600} 0.05 into 4x100 mL SOB medium pre-warmed to 50°C and incubated at 50°C and 200 RPM until OD_{600} 0.25. The cultures were transferred to 50 mL tubes and centrifuged at 7830 RPM and 25°C for ten minutes. The supernatant was discarded and the cells were resuspended in 4.5 mL electroporation buffer (EPB). The cell suspension from two and two tubes were combined and centrifuged at 7830 RPM and 25°C for ten minutes. The supernatant was discarded and the cells were gently resuspended in 9 mL EPB, and centrifuged at 7830 RPM and 25°C for ten minutes. The supernatant was discarded and the cells were resuspended in remaining EPB. All tubes were finally combined and 100 µL aliquots were prepared, these were stored at -80°C.

2) Transformation by electroporation:

Electrocompetent *B. methanolicus* MGA3 cells were transformed by electroporation. Plasmid DNA (0.5-1.0 µg) was added to 100 µL electrocompetent cells and transferred to cold electroporation cuvettes (0.2 cm), these were incubated on ice for 30 minutes. Electroporation was performed using the Gene Pulser Xcell Electroporation System (Bio-Rad) according to Table 2.7. Immediately after electroporation, 1 mL SOB medium pre-warmed to 50°C was added to the cuvette, pipetted up and down and transferred to 12.5 mL SOB pre-warmed to 50°C. The cells were incubated at 50°C and 200 RPM for 5-6 hours. Cells were harvested by centrifugation at 7830 RPM and 25°C for five minutes, the cells were resuspended in 100 µL SOB medium and plated on SOB plates supplemented with appropriate antibiotics. The plates were incubated at 50°C overnight.

Table 2.7: Gene Pulser Xcell Electroporation System settings for transformation of *B. methanolicus* MGA3

Resistance	200 Ω
Capacitance	25 µF
Voltage	12.5 kV/cm (2.5kV)
Time constant	4.5-5.5

Fresh colonies were picked and inoculated in 12.5 mL MVcMY medium supplemented with appropriate antibiotics and incubated at 50°C and 200 RPM overnight. The cultures were incubated until OD_{600} 2.0-2.5 (cultures were re-inoculated if $OD_{600}>2.5$). Three millilitres 89% glycerol was added to 9 mL of grown culture and 1 mL aliquots were prepared and stored at -80°C.

3) Transformation by conjugation:

E. coli S17-1 was transformed with plasmid of interest via heat shock as described in Section 2.2-7. Pre-cultures of *B. methanolicus* MGA3 recipient strains and *E. coli* S17-1 donor strains were incubated in 20 mL SOB medium and 10 mL LB medium, respectively, supplemented with appropriate antibiotics, overnight. Pre-cultures were re-inoculated to OD_{600} 0.05 into 10 mL non-selective SOB medium pre-warmed to 50°C and 10 mL selective LB medium for *B. methanolicus* MGA3 and *E. coli* S17-1, respectively, and the cultures were incubated for four hours. The cultures were cooled down to room temperature and mixed in two different amounts; 900 µL MGA3 with 300 µL S17-1, and 9 mL MGA3 with 3 mL S17-1. The mixtures were centrifuged at 16000 RPM and 25°C for five minutes, the cells were resuspended and dropped on non-selective SOB plates pre-warmed to 40°C and incubated at 40°C overnight.

The cells were scraped off and resuspended in 200 µL non-selective LB medium pre-warmed to 50°C. The suspension was diluted 10x, both undiluted and the 1:10 dilution were plated on SOB plates supplemented with appropriate antibiotics and incubated at 50°C overnight.

Fresh colonies were inoculated in both 10 and 20 mL SOB medium and MVcMY medium and incubated at 50°C and 200 RPM overnight. Glycerol stocks were prepared and stored at -80°C.

4. Growth experiments of recombinant B. methanolicus MGA3 strains

Pre-cultures of recombinant *B. methanolicus* MGA3 strains, as well as empty-vector control strains, were inoculated in 40 mL MVcMY medium supplemented with appropriate antibiotics at optimal times and incubated at 50°C and 200 RPM overnight. Required pre-culture volume for inoculation of main cultures to OD_{600} 0.2 was calculated and four times the required volume was centrifuged at 4000 RPM and 40°C for five minutes. The supernatant was discarded and the cells were resuspended in 4 mL MVcM medium pre-warmed to 50°C (without carbon source). Three main culture flasks containing 20 mL MVcM medium pre-warmed to 50°C were inoculated with 1 mL of prepared pre-culture inoculum and incubated

at 50°C and 200 RPM for 48 hours. OD_{600} measurements were routinely performed and samples for HPLC were routinely harvested.

5. Analyses of products by high pressure liquid chromatography (HPLC)

1) Violacein detection:

HPLC samples were harvested by centrifuging 500 µL of culture and transferring the supernatant to clean tubes, both the tubes containing the supernatant and pellet were stored at -20°C. Final preparation of HPLC samples was performed by thoroughly resuspending the pellets in 500 µL HPLC-grade MeOH and incubating the mixture at 30°C for 24 hours. The suspensions were then centrifuged at 13000 RPM and 25°C for five minutes and the supernatant was transferred to clean tubes and stored at 4°C. The HPLC protocol for detection and quantification of violacein was adapted from Tong *et al*. [69]. Quantification of violacein was performed on Alliance e2695 XE HPLC System (Waters®) using Waters Symmetry C18 Column (100 Å, 3.5 µm, 4.6 mm x 75 mm) equipped with 2489 UV/Visible detector (Waters®) at 254 nm. Mobile phase A of 0.1% acetic acid in MeOH (v/v) and B of 0.1% acetic acid in MilliQ H_2O (v/v) were utilised by gradient elution at a flow rate of 0.4 mL/minute at 25°C and 4000 psi. Violacein was quantified using a standard curve of 12.5 mg/L, 25 mg/L, 50 mg/L and 100 mg/L prepared from commercial violacein standard from J. lividum (>98% crude violacein for HPLC) diluted in MeOH.

2) Indole detection:

The HPLC protocol for detection and quantification of indole was adapted from Pérez-García *et al*. [70]. Samples were derivatised with fluorenylmethyl chloroformate (FMOC). Quantification of indole was carried out on Alliance e2695 XE HPLC System (Waters®) using Waters Symmetry C18 Column (100 Å, 3.5 µm, 4.6 mm x 75 mm) and 2475 Fluorescence (FLR) Detector (Waters®) at excitation 230 nm and emission 310 nm, accordingly. Mobile phase A of MeOH and B of 0.1 M sodium acetate (VWR®), pH 4.2 (with 0.025% sodium azide) at a flow rate of 1.3 mL/minute, 40°C and 4000 psi. Indole was quantified using a standard curve of 12.5 mg/L, 25 mg/L, 50 mg/L, 100 mg/L and 200 mg/L of indole prepared from commercial standard diluted in MilliQ H_2O.

3. Results

1. Methanol-based production of violacein

1) Construction of systems for combinatorial plasmid-based expression of vio genes:

Genomic DNA was isolated from *C. violaceum* MK and the *vioABCDE* genes were amplified by PCR. Nine DNA fragments were amplified. The genes *vioABC* and *vioE* were to be assembled as pBV2xp-*vioABCE*. *vioA*, *vioC* and *vioD* were to be assembled as pBV2xp-*vioACD*. *vioB* and *vioE* were to be assembled as pNW33Nmp-*vioBE*. *vioD* and *vioE* were amplified with another set of primers to be assembled as pNW33Nmp-*vioD* and pNW33Nmp-*vioE*, respectively. Each DNA fragment was purified and visualised by agarose gel electrophoresis, as shown in Figure 3.1.

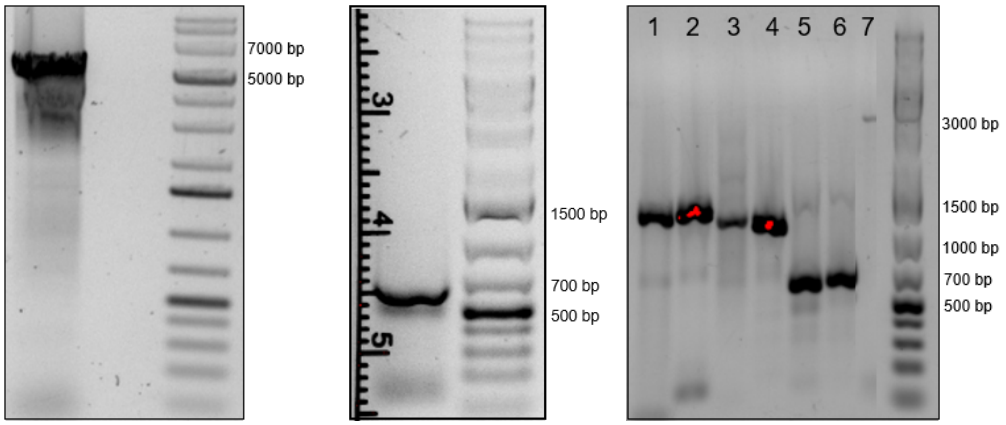

(a) (b) (c)

Fig. 3.1: Results from agarose gel electrophoresis of purified DNA fragments derived from the *C. violaceum* MK *vioABCDE* operon, amplified by PCR. (a) *vioABC*, (b) *vioE* (for *vioABCE*), (c-1) *vioA*, (c-2) *vioC*, (c-3) *vioD* (for *vioACD*), (c-4) *vioD*, (c-5) *vioE*, (c-6) *vioE* (for *vioBE*) and (c-7) *vioB*. Fragment sizes: *vioABC*: 5619 bp; *vioE*: 576 bp; *vioA*: 1257 bp; *vioC*: 1290 bp; *vioD*: 1122 bp; *vioB*: 2997 bp. The marker used is GeneRuler 1kb Plus DNA Ladder (Thermo Scientific™).

The plasmids pBV2xp and pNW33Nmp were isolated from *E. coli* and digested with restriction enzymes *Bam*HI (only for pBV2xp) and *Sac*I. The plasmids were purified and confirmed by agarose gel electrophoresis as shown in Figure 3.2.

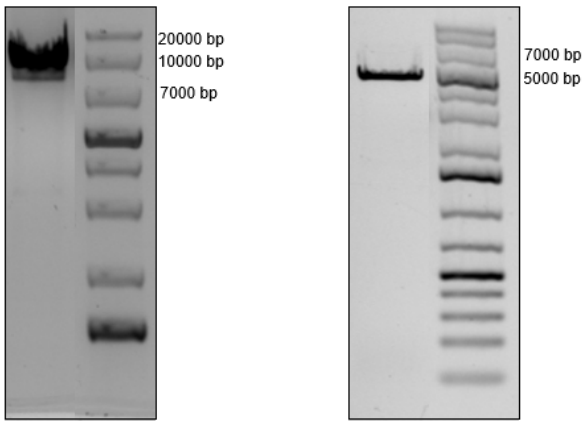

(a) (b)

Fig. 3.2: Results from agarose gel electrophoresis of plasmids digested with restriction enzymes. (a) pBV2xp digested with *Bam*HI and *Sac*I, (b) pNW33Nmp digested with *Bam*HI. Fragment sizes: pBV2xp: 8104 bp; pNW33Nmp: 5306 bp. The marker used is GeneRuler 1kb Plus DNA Ladder (Thermo Scientific™).

The DNA fragments and prepared plasmids were assembled for transformation and heterologous expression in *B. methanolicus* MGA3 via the Gibson assembly method, these plasmids are given in Figure 3.3.

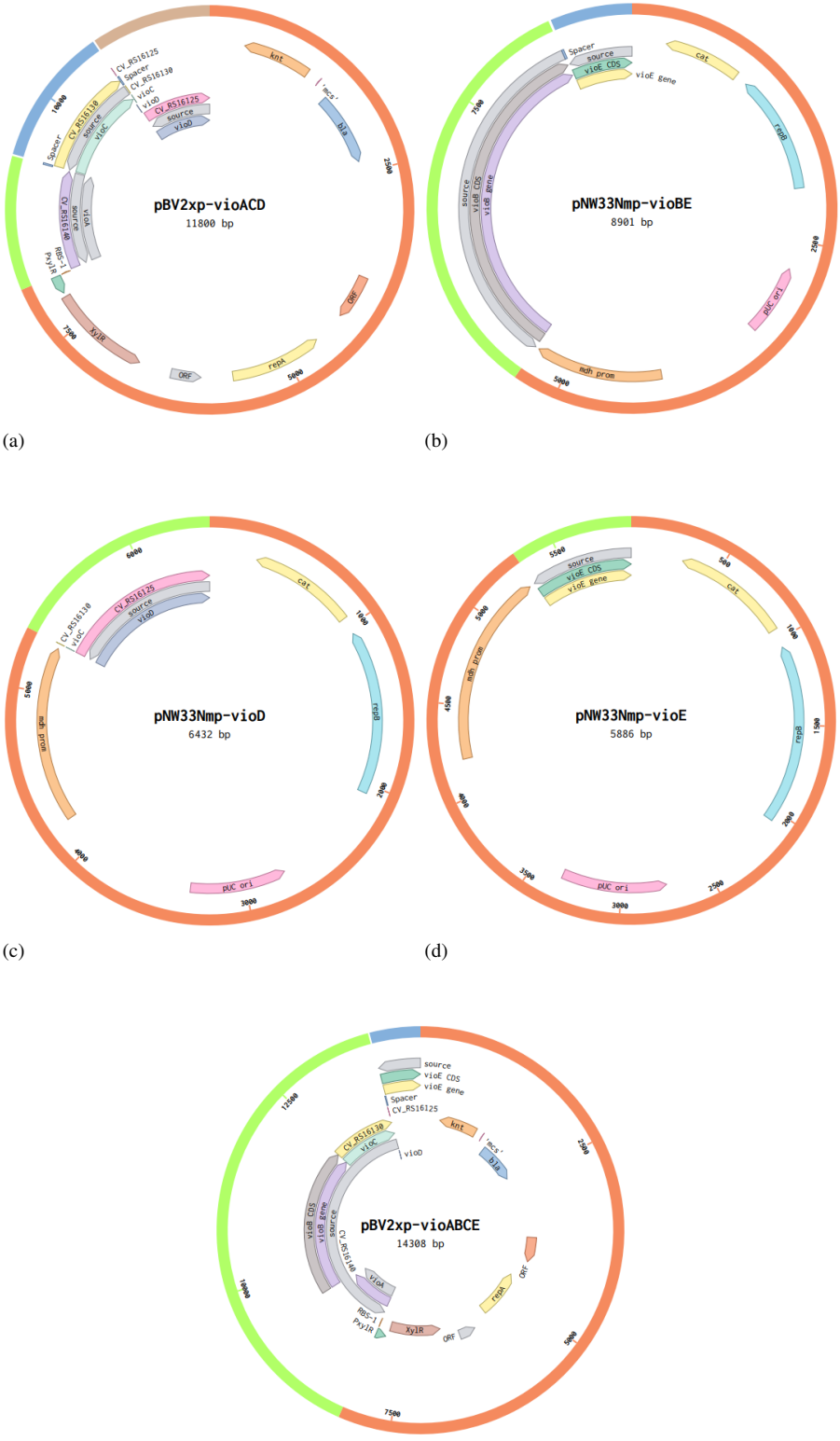

Fig. 3.3: Plasmid maps of expression systems (a) pBV2xp-*vioACD*, (b) pNW33Nmp-*vioBE*, (c) pNW33Nmp-*vioD*, (d) pNW33Nmp-*vioE* and (e) pBV2xp-*vioABCE*.

E. coli DH5α was transformed with each plasmid and cPCR was performed on single colonies, positive clones were visualised by agarose gel electrophoresis as seen in Figure 3.4. Due to the size of the *vioACD* construct, the plasmid was isolated from the cloning host *E. coli* DH5α and digested with the restriction enzymes *Sac*I and *Xal*I for easier visualisation on the agarose gel (Figure 3.4a). After confirmation by agarose gel electrophoresis, the positive clones were stored as glycerol stocks at -80°C. The plasmids were isolated and prepared for sequencing. Sequencing results verified the nucleotide sequence of the constructs. Positive clones with pBV2xp-*vioABCE* were not obtained.

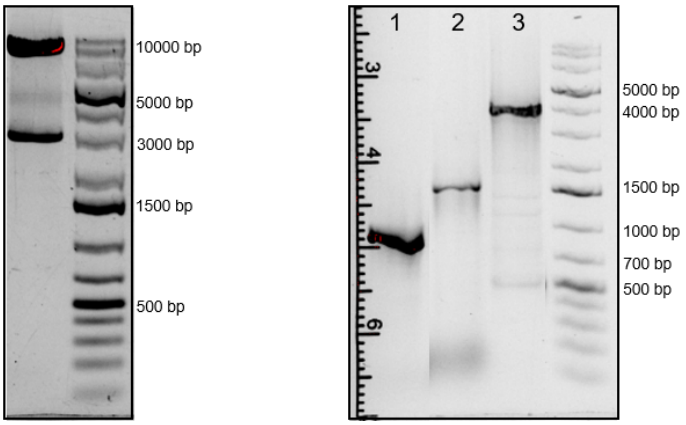

(a) (b)

Fig. 3.4: Results from agarose gel electrophoresis of plasmids harbouring (a) *vioACD*, (b-1) *vioE*, (b-2) *vioD* and (b-3) *vioBE*. pBV2xp-*vioACD* was digested with restriction enzymes prior to electrophoresis for better visualisation on the gel. Fragment sizes: pNW33Nmp-*vioE*: 1063 bp; pNW33Nmp-*vioD*: 1609 bp; pNW33Nmp-*vioBE*: 4078 bp; pBV2xp-*vioACD*: 8832 bp and 2968 bp. The marker used is GeneRuler 1kb Plus DNA Ladder (Thermo Scientific™).

2) Construction of systems for combinatorial plasmid-based expression of RBS-optimised vio genes:
The *C. violaceum* violacein biosynthetic operon with *B. methanolicus* RBS inserted upstream of each gene was amplified by PCR, purified and visualised by agarose gel electrophoresis as shown in Figure 3.5. The operon was amplified as two fragments *vioAB* (1) and *vioCDE* (2), and as one fragment *vioABCDE* (3).

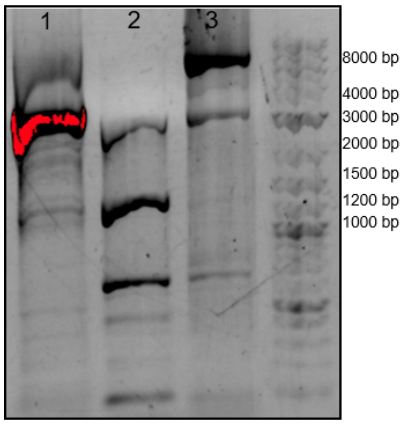

Fig. 3.5: Results from agarose gel electrophoresis of purified DNA fragments derived from the *C. violaceum* MK *vioABCDE* operon with *B. methanolicus* RBS inserted upstream of each gene. DNA fragments are amplified by PCR. Fragment sizes: *vioAB*-RBS: 4254 bp; *vioCDE*-RBS: 2988 bp; *vioABCDE*-RBS: 7242 bp. The marker used is 1kb Plus DNA Ladder (NEB).

The DNA fragments and prepared plasmids were assembled for transformation and heterologous expression in *B. methanolicus* MGA3 via the Gibson assembly method, this plasmid is given in Figure 3.6. Transformation in *E. coli* DH5α with the assembled plasmids was attempted, but no positive clones were obtained.

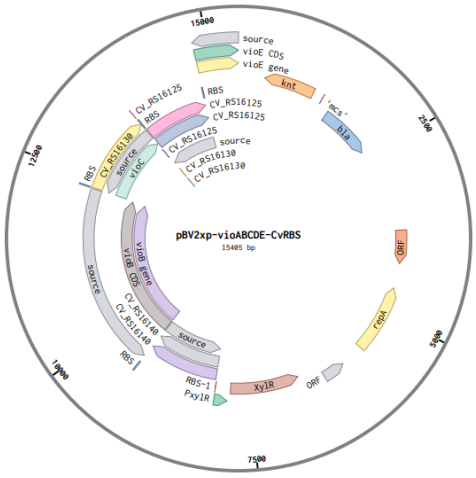

Fig. 3.6: Plasmid map of expression system pBV2xp-*vioABCDE*-RBS.

3) Growth of recombinant B. methanolicus MGA3 vio strains:

The constructed violacein biosynthesis expression vectors were transformed in *B. methanolicus* MGA3. A series of growth experiments were conducted for constructed recombinant strain *B. methanolicus* MGA3(pBV2xp-*vioACD*)(pNW33Nmp-*vioBE*) along with the respective empty vector controls. The empty vector controls are shown separately rather than as double transformants because double transformation was unsuccessful. Growth experiments with MGA3(pBV2xp-*vioABCDE*) were also conducted for comparison. The results of these experiments are plotted in Figure 3.7. The raw data can be found in Appendix C. Plots show the average values of triplicates, with the exception of Figure 3.7b, where two replicates of pBV are excluded from the calculations due to insufficient growth. Samples were regularly harvested and prepared for HPLC analysis, no positive HPLC results were obtained for any condition (data not shown).

(a)

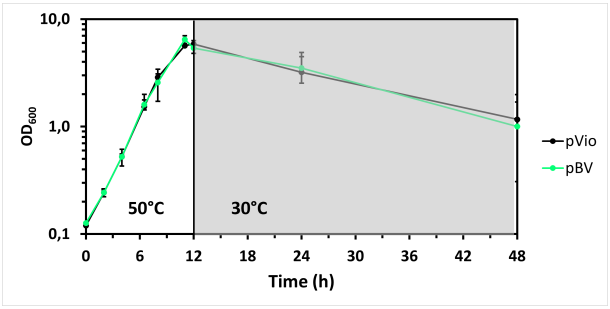

(b)

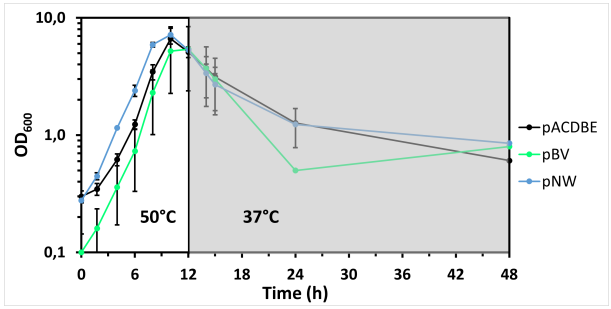

Fig. 3.7: Results from growth experiments of recombinant *B. methanolicus* MGA3 strains along with their empty vector controls, raw data can be found in Appendix C. The cultures were cultivated at 50 °C for the first 12h, then transferred to 30 or 37 °C (shaded area). Abbreviations: pBV: *B. methanolicus* MGA3(pBV2xp); pNW: *B. methanolicus* MGA3(pNW33Nmp); pVio: *B. methanolicus* MGA3(pBV2xp-*vioABCDE*); pACDBE: *B. methanolicus* MGA3(pBV2xp-*vioACD*)(pNW33Nmp-*vioBE*).

The exponential growth phase was determined to last for 10-12h depending on the strain. Calculated growth rates and doubling times of each strain, together with their maximal OD_{600} values, are reported in Table 3.1.

Table 3.1: Growth rates, doubling times and maximal OD_{600} values of constructed *B. methanolicus* MGA3 strains.

Strain	Growth rate (h^{-1})	Doubling time (h)	Maximal OD_{600}
pBV	0.36 ± 0.01	1.9	6.5 ± 0.6
pNW	0.35 ± 0.10	2.0	7.0 ± 1.0
pVio	0.37 ± 0.01	1.9	5.7 ± 0.6
pACDBE	0.33 ± 0.01	2.1	6.6 ± 0.2

pBV: *B. methanolicus* MGA3(pBV2xp)
pNW: *B. methanolicus* MGA3(pNW33Nmp)
pVio: *B. methanolicus* MGA3(pBV2xp-*vioABCDE*)
pACDBE: *B. methanolicus* MGA3(pBV2xp-*vioACD*)(pNW33Nmp-*vioBE*)

2. Methanol-based production of indole

1) Construction of systems for plasmid-based expression of tnaA:

Genomic DNA was isolated from *E. coli* K-12 and the *tnaA* gene was amplified by PCR, purified and visualised by agarose gel electrophoresis, as shown in Figure 3.8. The plasmid pUB110Sxp was digested with restriction enzymes *Bam*HI and *Sac*I and purified.

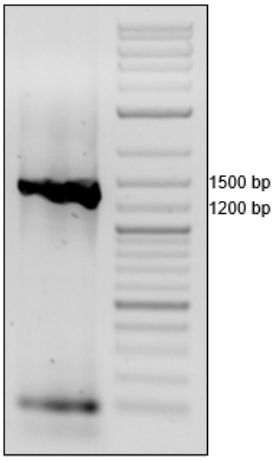

Fig. 3.8: Results from agarose gel electrophoresis of purified *tnaA* from *E. coli* K-12. Fragment size: 1416 bp. The marker used is 1kb Plus DNA Ladder (NEB).

The DNA fragment and prepared plasmid were assembled for transformation and heterologous expression in *B. methanolicus* MGA3 via the Gibson assembly method, this plasmid is given in Figure 3.9.

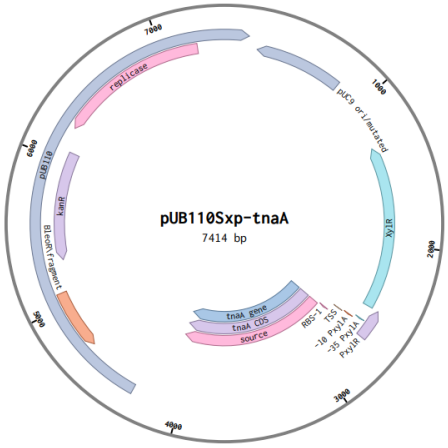

Fig. 3.9: Plasmid map of expression system pUB110Sxp-*tnaA*

E. coli DH5α was transformed with the constructed plasmid and cPCR was performed on single colonies, positive clones were visualised by agarose gel electrophoresis as shown in Figure 3.10. After confirmation by agarose gel electrophoresis, the positive clones were stored as glycerol stocks at -80°C. The plasmid was isolated and prepared for sequencing. Sequencing results verified the nucleotide sequence of the desired construct.

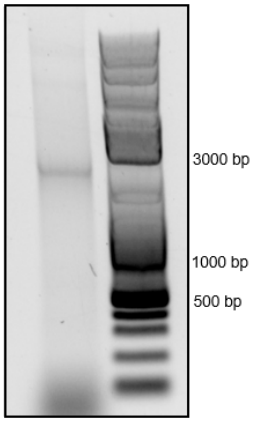

Fig. 3.10: Results from agarose gel electrophoresis of plasmid harbouring *tnaA*. Fragment size: 1957 bp. The marker used is 1kb Plus DNA Ladder (NEB).

2) Growth of recombinant B. methanolicus MGA3 tnaA-strain:

The pUB110Sxp-*tnaA* plasmid was transformed in previously constructed *B. methanolicus* MGA3(pTH1mp-Trp3). A growth experiment was conducted for the constructed recombinant strain *B. methanolicus* MGA(pTH1mp-Trp3)(pUB110Sxp-*tnaA*) along with its empty vector controls. The empty vector controls are shown separately rather than as double transformants because double transformation was unsuccessful. The pTH1mp empty vector control is not shown due to insufficient growth. The raw data can be found in Appendix C, with the data plotted in Figure 3.11. Plots show the average values of triplicates.

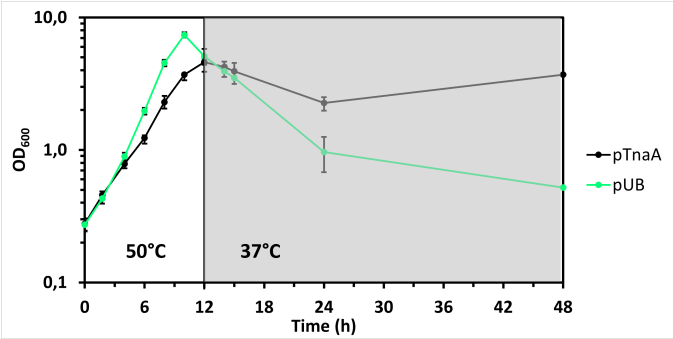

Fig. 3.11: Results from growth experiment of recombinant *B. methanolicus* MGA3 strains along with empty vector control, raw data can be found in Appendix C. The cultures were cultivated at 50 °C for the first 12h, then transferred to 37 °C (shaded area). Abbreviations: pUB: *B. methanolicus* MGA3(pUB110Sxp); pTnaA: *B. methanolicus* MGA3(pTH1mp-Trp3)(pUB110Sxp-*tnaA*).

The exponential growth phase was determined to last for 12h. Calculated growth rates and doubling times of each strain, together with their maximal OD_{600} values, are reported in Table 3.2.

Table 3.2: Growth rates, doubling times and maximal OD_{600} values of constructed *B. methanolicus* MGA3 strains.

Strain	Growth rate (h^{-1})	Doubling time (h)	Maximal OD_{600}
pUB	0.35 ± 0.01	2.0	7.4 ± 0.4
pTnaA	0.26 ± 0.01	2.7	4.6 ± 0.3

pUB: *B. methanolicus* MGA3(pUB110Sxp)
pTnaA: *B. methanolicus* MGA3(pTH1mp-Trp3)(pUB110Sxp-*tnaA*)

Samples were regularly harvested and prepared for HPLC analysis, no positive HPLC results were obtained for any condition. Upon harvesting of samples for further analyses, *B. methanolicus* MGA3(pUB110Sxp) and *B. methanolicus* MGA3(pTH1mp-Trp3)(pUB110Sxp-*tnaA*) displayed a difference in colour after 48h of cultivation as shown in Figure 3.12.

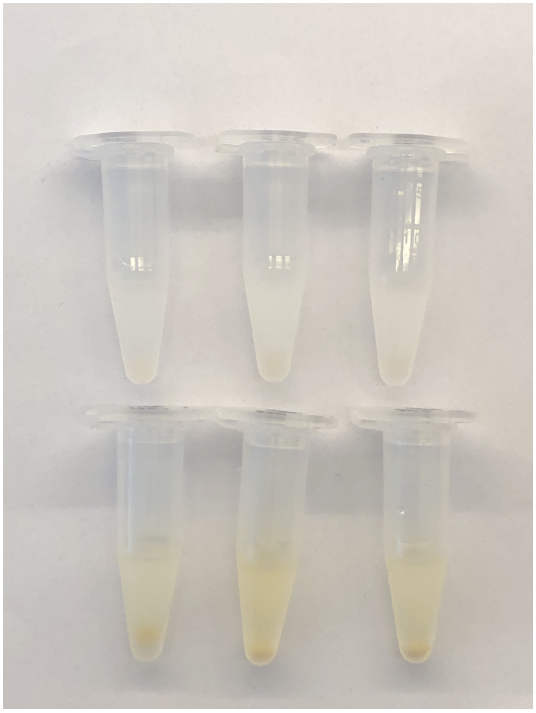

Fig. 3.12: Comparison of harvested samples of *B. methanolicus* MGA3(pUB110Sxp) (top) and *B. methanolicus* MGA3(pTH1mp-Trp3)(pUB110Sxp-*tnaA*) (bottom), all taken after 48h of cultivation.

3. Methanol-based production of tryptamine

1) Construction of systems for plasmid-based expression of PP_2552:

Genomic DNA was isolated from *P. putida* KT2440 and the PP_2552 gene was amplified by PCR, purified and visualised by agarose gel electrophoresis, as shown in Figure 3.13. The plasmid pUB110Sxp was digested with restriction enzymes *Bam*HI and *Sac*I and purified.

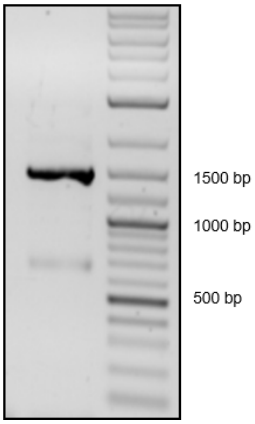

Fig. 3.13: Results from agarose gel electrophoresis of purified PP_2552 from *P. putida* KT2440. Fragment size: 1413 bp. The marker used is 1kb Plus DNA Ladder (NEB).

The DNA fragment and prepared plasmid were assembled for transformation and heterologous expression in *B. methanolicus* MGA3 via the Gibson assembly method, this plasmid is given in Figure 3.14. This plasmid was not constructed in this study.

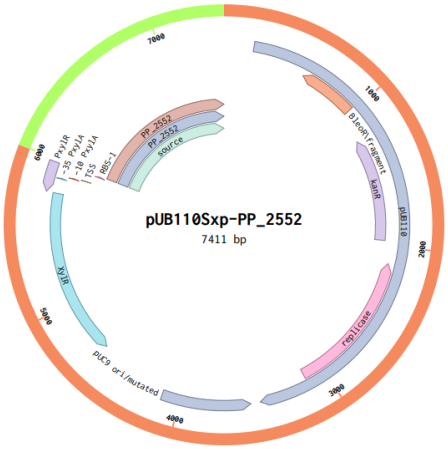

Fig. 3.14: Plasmid map of expression system pUB110Sxp-PP_2552

4. Discussion

1. Violacein production in B. methanolicus MGA3

1) Strategies for optimisation of violacein production:

Several combinations of genes from the *vio* operon were constructed as seen in Figure 3.3. These combinations were designed with the goal of optimising violacein production by solving potential bottleneck problems. The biosynthesis pathway of violacein depends heavily on VioE to convert the IPA imine dimer to protodeoxyviolaceinic acid rather than the spontaneous, irreversible formation of chromopyrrolic acid. Should the amount of VioE present be insufficient, it would decrease the final violacein yield as large parts of Trp would go to waste as chromopyrrolic acid. *E. coli* has been engineered for overexpression of VioE, resulting in a crude violacein titer of 4.45 g/L in fed-batch fermentation, an increase from previously reported titers of 0.71 and 1.75 g/L in *E. coli* [71].

Another important enzyme for optimisation of violacein yield is VioD, which is responsible for the hydroxylation of protodeoxyviolaceinic acid. With insufficient amounts of VioD, the result would be an impure product consisting of both violacein and deoxyviolacein. Titers of pure violacein of 0.71 g/L have been reported in recombinant *E. coli* strains [72].

VioB has previously been identified as the rate limiting step in violacein production [73], catalysing the reaction between two Trp molecules to form the IPA imine dimer. Overexpression of VioB is therefore another potential strategy, however, increased synthesis rate of the IPA imine dimer would also require additional increased levels of VioE in order to avoid formation of chromopyrrolic acid, thus, overexpression of VioBE was also targeted as a strategy.

Finally, violacein has been produced by engineered *C. glutamicum* at a titer of 5.44 g/L in fed-batch fermentation. This titer was improved from 0.5 g/L by replacing the native RBS of the *C. violaceum* donor with strong *C. glutamicum* RBS [74]. Another strategy therefore is to insert *B. methanolicus* RBS upstream of each *vio* gene.

All strategies envisioned in this study are listed in Table 4.1. The genes to be overexpressed are carried on the pNW33Nmp plasmid. This is a RC replicating, high copy number plasmid with a long history of use in *B. methanolicus* MGA3 [21, 63].

Table 4.1: Envisioned strategies for optimisation of violacein production in *B. methanolicus* MGA3

Strategy	Description	Ref.
1	*B. methanolicus* MGA3(pBV2xp-*vioABCDE*)(pNW33Nmp-*vioD*)	[72]
2	*B. methanolicus* MGA3(pBV2xp-*vioABCDE*)(pNW33Nmp-*vioE*)	[71]
3	*B. methanolicus* MGA3(pBV2xp-*vioABCE*)(pNW33Nmp-*vioD*)	[72]
4	*B. methanolicus* MGA3(pBV2xp-*vioACD*)(pNW33Nmp-*vioBE*)	[73]
5	*B. methanolicus* MGA3(pBV2xp-*vioABCDE*)-RBS	[74]

2) Construction of expression vectors for violacein production:

The *vio* genes were amplified from *C. violaceum* gDNA by PCR and assembled as expression vectors listed above. Construction of the expression vector pBV2xp-*vioABCE* for strategy 3 proved difficult and this plasmid was not constructed in this study. Amplification of *vioABC* and *vioE*, using primers listed in Table A.1, was successful. As seen in Figure 3.1a and 3.1b, the acquired DNA fragments are of desired size, the problem therefore is thought to lie in the transformation efficiency of this particular plasmid. This expression system is based on pBV2xp, which already resulted in successful insertion of *vioACD* in *E. coli* DH5α, verified by sequencing, proving the method works. The transformation protocol was repeated several times with the same conditions as for *vioACD* in order to acquire positive *E. coli* DH5α clones harbouring pBV2xp-*vioABCE* without success. This is a slightly larger plasmid than pBV2xp-*vioACD*, by around 2500 bp, and transformation efficiency has been reported to decrease by increasing plasmid size [64]. However, there is only a very marginal difference in efficiency between plasmids of 10 and 20 kb, therefore, plasmid size is not likely to be the main cause of the issue presented here.

Another theory is a high frequency of recircularisation of the cloning vector without the gene insert. As colonies were acquired after most transformation attempts, transformation of the pBV2xp plasmid carrying the *knt* gene conferring kanamycin resistance, with or without insertion of *vioABCE*, had to have taken place in order for the colonies to grow on plates supplemented with kanamycin. Attempts at dephosphorylisation of the plasmid were made to avoid recircularisation of the plasmid without the insert. This method did not result in any greater transformation efficiency. It should be said that not every single colony on each plate was tested, and although the vast majority were, there always remains a chance that some of the untested colonies did indeed contain a successfully inserted *vioABCE* sequence. Additional transformations were performed, but with equally unsuccessful results.

More work is nevertheless required for this particular expression system, either by conducting the same experiments until a positive clone is detected or by attempting alternative ways of transforming *E. coli* DH5α. First of all, some parameters of the heat shock protocol could be altered, such as the duration and temperature of the heat shock or incubation conditions. Secondly, utilising chemical methods is common for bacterial transformations. Here, $CaCl_2$ is used to counteract the electrostatic repulsion between plasmid DNA and the cellular membrane of the bacteria thanks to the Ca^{2+} ions [75].

Other methods of transformation include Hanahan's method [64] and the DMSO method [75]. More recent alternative approaches have been reported to increase transformation efficiency in *E. coli* by using silver nanoparticles [76] and magnesium aminoclays [77, 78, 79].

A previous study started developing plasmids harbouring the *vioABCDE* operon of *C. violaceum* with an RBS for *B. methanolicus* upstream of each gene [65]. Stronger ribosome binding increases translation efficiency of the mRNA and a study utilising optimised RBS sequences has led to titers of 5.44 g/L violacein in *C. glutamicum* [74]. Optimised RBS have also shown to increase the functional temperature of the violacein biosynthetic enzymes [80]. Another aim of this study was thus to continue the construction of RBS-optimised *vio* genes using gene splicing by overlap extension PCR ("gene SOEing"), and subsequent transformation of constructed plasmids in *B. methanolicus* MGA3. As the *vio* operon is quite large, two strategies for "gene SOEing" were envisioned; amplification of the entire operon as one fragment (7242 bp) and separated into *vioAB* (4254 bp) and *vioCDE* (2988 bp). Amplification of these fragments was successful as seen in Figure 3.5. The gel shows impure products consisting of multiple DNA fragments of different sizes, but this was to be expected from OE-PCR as there is no way to control which DNA fragments anneal to each other. The presence of bands at around 3000-4000 bp in the lanes of *vioAB* and *vioCDE* indicate successful amplification, likewise with a band around 7000-8000 bp in the lane of *vioABCDE*. These PCR products were purified, and assembly of linearised plasmid and DNA fragments was performed following the Gibson assembly method with pBV2xp as expression vector. As was the case with the transformation of *vioABCE*, however, transformation in *E. coli* DH5α was unsuccessful in this study.

3) Growth of violacein producing B. methanolicus MGA3 strains:

As mentioned, the expression vectors pBV2xp-*vioABCE* and pBV2xp-*vioABCDE*-RBS were not constructed in this study, and strategies 3 and 5 in Table 4.1 were therefore not ready to be tested. All remaining expression vectors were constructed, and transformation in *B. methanolicus* MGA3 was performed by two different methods with varying success: electroporation and conjugation, the latter using *E. coli* S17-1 as donor strain. Electroporation led to the successful construction of *B. methanolicus* MGA3(pBV2xp-*vioACD*), *B. methanolicus* MGA3(pNW33Nmp-*vioBE*) and *B. methanolicus* MGA3(pNW33Nmp-*vioD*), while *B. methanolicus* MGA3(pNW33Nmp-*vioE*) was constructed by conjugation. Additionally, all constructed plasmids were successfully transformed in *E. coli* S17-1 by the heat shock method.

Each recombinant *B. methanolicus* MGA3 strain was then to be additionally transformed with a compatible expression system according to the strategies in Table 4.1. The strain *B. methanolicus* MGA3(pBV2xp-*vioABCDE*), expressing the full violacein biosynthetic operon, was already available in the lab from a previous study [65]. Conjugation was the primary method used to create these double transformants as greater success had been reported by this method when the recipient strain already contains a foreign plasmid. Most attempts of conjugation were unsuccessful in this study, with the exception of strain *B. methanolicus* MGA3(pBV2xp-*vioACD*)(pNW33Nmp-*vioBE*) (strategy 4). The construction of *B. methanolicus* MGA3(pBV2xp)(pNW33Nmp) as a control during growth experiments was also attempted, but not accomplished. However, *B. methanolicus* MGA3(pBV2xp) and MGA3(pNW33Nmp) were created and used as two separate control strains.

Cultivation of *B. methanolicus* MGA3(pBV2xp-*vioACD*)(pNW33Nmp-*vioBE*) was performed to analyse the growth behaviour of this strain, however, no violacein was detected (data not shown). A previous study conducted in the same lab which established the basis of this work, i.e. by constructing the *B. methanolicus* MGA3(pBV2xp-*vioABCDE*) strain, was also unable to produce any violacein [65]. Their initial hypothesis was that a lack of Trp in the cells prevented violacein production, growth experiments with supplemental Trp additions to the growth media were then performed, but to no avail. Adding Trp to the media was not enough, possibly due to the fact that there is not a known importer for Trp in *B. methanolicus* [65]. Furthermore, it has been reported that violacein synthesis is negatively affected by increasing cultivation temperatures, even 37°C drastically decreases the violacein yield [72, 74]. This leads to the assumption that the 50°C growth temperature of *B. methanolicus* is a significant obstacle to violacein production. The cited studies were carried out in *C. glutamicum* and *E. coli*, both of which grow at 37°C as further proven by reported biomass yields [72, 74], the temperature should therefore not affect the host organisms' metabolic abilities. This further strengthens the assumption that temperature is the primary cause of poor violacein production, with the higher temperature likely causing stability or folding problems of the Vio enzymes [72].

Attempts to overcome the temperature obstacle were conducted by transferring the *B. methanolicus* MGA3 cultures to 30 and 37°C after 12h of cultivation at 50°C. The exponential growth phase of each constructed recombinant strain lasts until 10-12h after inoculation (Figure 3.7), biomass should therefore be at a peak around this time and the transfer to lower temperatures would hopefully allow for increased activity of the Vio enzymes. Still, no production was achieved, both indicated by the colour of the cultures being no different than the empty vector control strains and by no violacein detection in HPLC measurements (data not shown). Two approaches were devised to achieve violacein production: improving the Trp supply in the cells and utilising RBS for *B. methanolicus* upstream of the genes.

4) Improving tryptophan supply in B. methanolicus MGA3:

A separate study conducted in parallel with the one presented in this report has explored and improved the supply of Trp in *B. methanolicus* MGA3. Trp is, as mentioned earlier, the common precursor to violacein, indole and tryptamine,

and a steady supply of Trp is of great interest when producing these compounds. Said study was able to construct the expression vector pTH1mp-Trp3 for use in *B. methanolicus* MGA3, which is able to produce titers of 0.2 g/L to date [45]. This vector consists of the *trpDGE* genes [45], encoding for anthranilate synthase components I and II and anthranilate phosphoribosyl transferase which are responsible for the conversion of chorismate to PRA [35, 36]. Production of violacein would hopefully be achieved By combining the violacein biosynthetic genes with Trp3 as the cells would have access to increased levels of Trp. Firstly, construction of the recombinant double transformant *B. methanolicus* MGA3(pTH1mp-Trp3)(pBV2xp-*vioABCDE*) was attempted in order to achieve violacein production, before combining pTH1mp-Trp3 with the strategies listed in Table 4.1. This transformation was attempted by conjugation, as both *B. methanolicus* MGA3(pTH1mp-Trp3) and the plasmid pBV2xp-*vioABCDE* had already been constructed in previous studies and the only task was to achieve co-expression. pBV2xp-*vioABCDE* was successfully transformed in *E. coli* S17-1 as the donor strain, however, further transformation in *B. methanolicus* MGA3 was not accomplished in this study. Until these *B. methanolicus* MGA3 strains are constructed, it will be difficult to determine the main factors affecting violacein synthesis. Further experimentation with the currently constructed strains could still prove useful, such as transferring the cultures to 30-37°C earlier in the exponential growth phase or assays for detection of Vio enzymes and related enzymatic activities.

5) RBS-optimised violacein biosynthetic genes:

It is unclear whether or not synthesis of the Vio enzymes took place at all, regardless of the temperature. If the enzymes were present and simply denatured due to temperature, lowering the temperature should renature them and restore their activity as denaturation is normally a reversible process [81]. One possibility is that the enzymes were not synthesised to begin with. As mentioned in Section 4.1-2, construction of the violacein biosynthetic operon with *B. methanolicus* RBS upstream of each gene was begun in a previous study [65], this project was continued in this study. Optimised RBS should facilitate violacein synthesis by increasing the translation efficiency of the mRNA and thereby increase the concentration of the enzymes, as well as improving the thermostability of the enzymes. The RBS-optimised *vio* operon was successfully amplified as mentioned in Section 4.1, and as can be seen in Figure 3.5, confirmed by DNA fragments of desired sizes. Construction of the expression vector pBV2xp-*vioABCDE*-RBS was not accomplished in this study as no positive *E. coli* DH5α clones were acquired. Once *B. methanolicus* MGA3(pBV2xp-*vioABCDE*)-RBS is constructed, co-expression with pTH1mp-Trp3 could a promising continuation to achieve and to later optimise violacein production.

2. Indole and tryptamine production in B. methanolicus MGA3

Indole and tryptamine were identified as alternative products arising from tryptophan metabolism. These two products are more closely derived from Trp and require only a single reaction step catalysed by tryptophanase and putative decarboxylase, respectively for indole and tryptamine. It was theorised that these biosynthesis pathways, being both simpler and more thermotolerant, would result in not only more straightforward transformations but also production of the target compounds. Two different forward primers were designed for amplification of PP_2552; mgl164 and mgl166, the latter exchanging the former's GTG start codon with ATG. As ATG is the most common start codon for translation [82], it would be interesting to see if the exchange of the gene's native GTG start codon with ATG would have an effect on increased translation rates. Unfortunately, similar problems as with *vioABCE* occured and transformation of *E. coli* DH5α with PP_2552 was not accomplished in this study. Likewise, further work on this is required to achieve successful transformations in *E. coli* DH5α and later in *B. methanolicus* MGA3. Molecular work on *tnaA* on the other hand led to positive *E. coli* DH5α clones verified by sequencing. The constructed plasmid pUB110Sxp-*tnaA* was then successfully transformed in *E. coli* S17-1, and the double transformant *B. methanolicus* MGA3(pTH1mp-Trp3)(pUB110Sxp-*tnaA*) was constructed by conjugation.

A growth experiment with *B. methanolicus* MGA3(pTH1mp-Trp3)(pUB110Sxp-*tnaA*) was conducted and the results are seen in Figure 3.11 and Table 3.2. Samples were harvested for analysis by HPLC, but the HPLC run did not work and as such, no HPLC results were acquired to verify the production of indole. Due to time constraints it was not possible to perform another HPLC run in this study. Nevertheless, as shown in Figure 3.12, there is a clearly distinct colour difference between cultures with the empty vector control strain and the strain harbouring the *tnaA* gene. Additionally, the growth rate of the empty vector control strain was 0.35 ± 0.01 h^{-1} compared to only 0.26 ± 0.01 h^{-1} for the *tnaA* strain. These two observations together are indicators of indole production, with the lower growth rate implying that the cells spent less energy on growth in order to fuel other metabolic paths, such as indole production. Indole also exhibits oxidant toxicity which inhibits bacterial growth [83], this can further help explain the lower growth rate and indicate indole production. Further HPLC analyses still need to be performed to verify the presence of indole in these samples to confirm production. The *tnaA* gene was combined with pTH1mp-Trp3 to increase Trp supply, and although *B. methanolicus* carries a chromosomal copy of *trpB*, catalysing the conversion of indole to Trp, the fact that this reaction is negligible as well as *tnaA* being located on a high copy number plasmid rather than being chromosomal should in theory lead to accumulation of indole. It is unclear how great an effect Trp3 has on the potential indole production as a *B. methanolicus* MGA3 strain harbouring solely the *tnaA* gene was not tested nor constructed. It has been reported that indole production in *E. coli*, although optimal at 37°C, still functions at up to 50°C [84]. Both of these factors could be the reason why indole production was potentially achieved whereas violacein production was not.

3. Future Work

This project has provided several takeaways that can be useful for future work. Progress was made for violacein production by constructing the recombinant strain *B. methanolicus* MGA3(pBV2xp-*vioACD*)(pNW33Nmp-*vioBE*) along with multiple expression vectors which can be transformed in *B. methanolicus* MGA3 in future projects. Further growth experiments and HPLC analyses should be conducted on both the strain constructed in this study and the remaining strains once constructed. The work on the RBS-optimised violacein biosynthetic operon and Trp3 are promising approaches which should be explored further.

Different microbial hosts for violacein production have been explored in previous studies, i.e. the mesophilic methylotroph *Methylobacterium extorquens* AM1 [6, 65]. This bacterium provides an alternative strategy for methanol-based production of violacein at temperatures where violacein production has been reported in the past [72, 74]. Although these studies in *M. extorquens* AM1 are yet to produce violacein, this could be worth exploring further.

The recombinant strain *B. methanolicus* MGA3(pTH1mp-Trp3)(pUB110Sxp-*tnaA*) was successfully constructed and showed indicators of indole production. Further HPLC analysis of this strain is however needed to verify the presence of indole. Additionally, constructing the strain *B. methanolicus* MGA3(pUB110Sxp-*tnaA*) would be of interest to observe the effect of Trp3 on indole production. This could provide further insight into its effect on other Trp-derived compounds.

Transformation of *B. methanolicus* MGA3 by electroporation achieved a higher success rate than conjugation in this study, both for the construction of single and double transformants, and should be considered the most promising method moving forward.

5. Conclusion

This study aimed to produce Trp-derived compounds violacein, indole and tryptamine in metabolically engineered *B. methanolicus* MGA3 using methanol as carbon source. Constructing recombinant strains of *B. methanolicus* MGA3 for violacein production has proven difficult and no violacein production was detected in this study. Two reasons have been hypothesised; temperature and lack of intracellular Trp. Efforts were made to overcome these obstacles by improving the Trp supply in the cells and utilising *B. methanolicus* RBS, these strategies require further work.

A recombinant strain of *B. methanolicus* MGA3 for indole production by *tnaA* was constructed and indications of indole production were observed, however, further analysis is required to verify the production of indole. Recombinant *B. methanolicus* MGA3 strains for tryptamine production were not constructed in this study and require further work.

Valuable insights into the potential of *B. methanolicus* as a production host for Trp-derived compounds have been gained in this study, which provide a stronger basis for future work on this topic. By solving the problems presented in this study and exploring the approaches proposed here, it will not only expand the range of products in *B. methanolicus*, but also contribute towards the use of other methylotrophic and thermophilic bacteria as production host for value-added compounds. Discovering new methods for methanol-based production of such compounds is of great interest in order to rival the use of sugar-based feedstocks.

REFERENCES

[1] D. S. Marlin, E. Sarron, and Ó. Sigurbjörnsson. "Process Advantages of Direct CO_2 to Methanol Synthesis". In: *Frontiers in Chemistry* 6 (2018). DOI: https://dx.doi.org/10.3389%2Ffchem.2018.00446.

[2] W. Zhang *et al*. "Metabolic Engineering of *Escherichia coli* for High Yield Production of Succinic Acid Driven by Methanol". In: *ACS Synthetic Biology* 7 (2018). DOI: https://doi.org/10.1021/acssynbio.8b00109.

[3] J. Pfeifenschneider, T. Brautaset, and F. W. Volker. "Methanol as carbon substrate in the bio-economy: Metabolic engineering of aerobic methylotrophic bacteria for production of value-added chemicals". In: *Biofuels, Bioproducts and Biorefining* 11 (2017). DOI: https://doi.org/10.1002/bbb.1773.

[4] J. Yang *et al*. "Metabolic engineering of *Methylobacterium extorquens* AM1 for the production of butadiene precursor". In: *Microbial Cell Factories* 17 (2018). DOI: https://doi.org/10.1186/s12934-018-1042-4.

[5] J. Schrader *et al*. "Methanol-based industrial biotechnology: current status and future perspectives of methylotrophic bacteria". In: *Trends in Biotechnology* 27 (2009). DOI: https://doi.org/10.1016/j.tibtech.2008.10.009.

[6] D. Korneliussen. "Establishment of *Methylobacterium extorquens* AM1 as host for methanol-based violacein production". Unpublished. 2021.

[7] T. Blumberg *et al*. "Methanol production from natural gas - a comparative exergoeconomic evaluation of commercially applied synthesis routes". In: July 2017.

[8] S. Gumber and A.V.P. Gurumoorthy. "Methanol: Science and Engineering". In: Elsevier, 2017. Chap. 25: Methanol Economy versus Hydrogen Economy. DOI: https://doi.org/10.1016/C2016-0-00366-2.

[9] H. Yurimoto *et al*. "Assimilation, dissimilation, and detoxification of formaldehyde, a central metabolic intermediate of methylotrophic metabolism". In: *The Chemical Record* 5 (2005). DOI: https://doi.org/10.1002/tcr.20056.

[10] F.H. Sobels. "Organic peroxides and mutagenic effects in *Drosophila*". In: *Nature* (1956). DOI: https://doi.org/10.1038/177979a0.

[11] M.C. Becerra *et al*. "Lipids and DNA oxidation in *Staphylococcus aureus* as a consequence of oxidative stress generated by ciprofloxacin". In: *Molecular and Cellular Biochemistry* 285 (2006). DOI: https://doi.org/10.1007/s11010-005-9051-0.

[12] W. Jiang *et al*. "Metabolic engineering strategies to enable microbial utilization of C1 feedstocks". In: *Nature Chemical Biology* 17 (2021). DOI: https://doi.org/10.1038/s41589-021-00836-0.

[13] J. Pfeifenschneider *et al*. "Transaldolase in *Bacillus methanolicus*: biochemical characterization and biologicalrole in ribulose monophosphate cycle". In: *BMC Microbiology* 20 (2020). DOI: https://doi.org/10.1186/s12866-020-01750-6.

[14] T. Brautaset *et al*. "*Bacillus methanolicus*: a candidate for industrial production of amino acids from methanol at 50°C". In: *Applied Microbiology and Biotechnology* 74 (2007). DOI: https://doi.org/10.1007/s00253-006-0757-z.

[15] J. Stolzenberger *et al*. "Characterization of fructose 1,6-bisphosphatase and sedoheptulose 1,7-bisphosphatase from the facultative ribulose monophosphate cycle methylotroph Bacillus methanolicus". In: *Journal of Bacteriology* 195 (2013). DOI: https://doi.org/10.1128/jb.00672-13.

[16] V.J. Klein *et al*. "Unravelling Formaldehyde Metabolism in Bacteria: Road towards Synthetic Methylotrophy". In: *Microorganisms* 10 (2022). DOI: https://doi.org/10.3390/microorganisms10020220.

[17] F.J. Schendel *et al*. "L-Lysine Production at 50 °C by Mutants of a Newly Isolated and Characterized Methylotrophic *Bacillus* sp." In: *Applied and Environmental Microbiology* (1990). DOI: https://doi.org/10.1128/aem.56.4.963-970.1990.

[18] M. Irla *et al*. "Complete genome sequence of *Bacillus methanolicus* MGA3, a thermotolerant amino acid producing methylotroph". In: *Journal of Biotechnology* 188 (2014). DOI: https://doi.org/10.1016/j.jbiotec.2014.08.013.

[19] Ø.M. Jakobsen *et al*. "Upregulated Transcription of Plasmid and Chromosomal Ribulose Monophosphate Pathway Genes Is Critical for Methanol Assimilation Rate and Methanol Tolerance in the Methylotrophic Bacterium *Bacillus methanolicus*". In: *Journal of Bacteriology* 188 (2006). DOI: https://doi.org/10.1128%2FJB.188.8.3063-3072.2006.

[20] A. Bozdag *et al*. "Growth of *Bacillus methanolicus* in 2 M methanol at 50 °C: the effect of high methanol concentration on gene regulation of enzymes involved in formaldehyde detoxification by the ribulose monophosphate pathway". In: *Journal of Industrial Microbiology and Biotechnology* 42 (2015). DOI: https://doi.org/10.1007/s10295-015-1623-8.

[21] M. Irla *et al*. "Genome-Based Genetic Tool Development for *Basillus methanolicus*: Theta- and Rolling Circle-Replicating Plasmids for Inducible Gene Expression and Application to Methanol-Based Cadaverine Production". In: *Frontiers in Microbiology* 7 (2016). DOI: https://doi.org/10.3389/fmicb.2016.01481.

[22] I. Nærdal *et al*. "Methanol-based cadaverine production by genetically engineered *Bacillus methanolicus* strains". In: *Microbial Biotechnology* 8 (2015). DOI: https://doi.org/10.1111/1751-7915.12257.

[23] M. Irla *et al*. "Methanol-based γ-aminobutyric acid (GABA) production by genetically engineered *Bacillus methanolicus* strains". In: *Industrial Crops and Products* 106 (2017). DOI: https://doi.org/10.1016/j.indcrop.2016.11.050.

[24] E. B. Drejer *et al*. "Methanol-based acetoin production by genetically engineered *Bacillus methanolicus*". In: *Green Chemistry* 22 (2020). DOI: https://doi.org/10.1039/C9GC03950C.

[25] L. F. Brito *et al*. "Evaluation of Heterologous Biosynthetic Pathways for Methanol-Based 5-Aminovalerate Production by Thermophilic *Bacillus methanolicus*". In: *Frontiers in Bioengineering and Biotechnology* 9 (2021). DOI: https://doi.org/10.3389/fbioe.2021.686319.

[26] K. Schultenkämper *et al*. "Establishment and application of CRISPR interference to affect sporulation, hydrogen peroxide detoxification, and mannitol catabolism in the methylotrophic thermophile *Bacillus methanolicus*". In: *Applied Microbiology and Biotechnology* 103 (2019). DOI: https://doi.org/10.1007/s00253-019-09907-8.

[27] I. Mougiakos *et al*. "Characterizing a thermostable Cas9 for bacterial genome editing and silencing". In: *Nature Communications* 8 (2017). DOI: https://dx.doi.org/10.1038%2Fs41467-017-01591-4.

[28] C.M. Santiveri and M.A. Jiménez. "Tryptophan residues: Scarce in proteins but strong stabilizers of β-hairpin peptides". In: *Peptide Science* 94 (2010). DOI: https://doi.org/10.1002/bip.21436.

[29] D.M. Richard *et al*. "L-Tryptophan: Basic Metabolic Functions, Behavioral Research and Therapeutic Indications". In: *International Journal of Tryptophan Research* 2 (2009). DOI: https://doi.org/10.4137%2Fijtr.s2129.

[30] A. Slominski *et al*. "Conversion of L-tryptophan to serotonin and melatonin in human melanoma cells". In: *FEBS Letters* 511 (2002). DOI: https://doi.org/10.1016/S0014-5793(01)03319-1.

[31] E. Merino *et al*. "Evolution of bacterial *trp* operons and their regulation". In: *Current Opinion in Microbiology* 11 (2008). DOI: https://doi.org/10.1016/j.mib.2008.02.005.

[32] A. Gutierrez-Preciado *et al*. "New insights into regulation of the tryptophan biosynthetic operon in Gram-positive bacteria". In: *Trends in Genetics* 21 (2005). DOI: https://doi.org/10.1016/j.tig.2005.06.001.

[33] F. Gibson. "The elusive branch-point compound of aromatic amino acid biosynthesis". In: *Trends in Biochemical Sciences* 24 (1999). DOI: https://doi.org/10.1016/S0968-0004(98)01330-9.

[34] K.M. Herrmann and L.M. Weaver. "The shikimate pathway". In: *Annual Review of Plant Physiology and Plant Molecular Biology* 50 (1999). DOI: https://doi.org/10.1146/annurev.arplant.50.1.473.

[35] A.A. Morollo and R. Bauerle. "Characterization of composite aminodeoxyisochorismate synthase and aminodeoxyisochorismate lyase activities of anthranilate synthase". In: *PNAS* 90 (1993). DOI: https://doi.org/10.1073/pnas.90.21.9983.

[36] C. Kim *et al*. "The crystal structure of anthranilate phosphoribosyltransferase from the enterobacterium *Pectobacterium carotovorum*". In: *FEBS Letters* 523 (2002). DOI: https://doi.org/10.1016/S0014-5793(02)02905-8.

[37] T.E. Creighton and C. Yanofsky. "Chorismate to tryptophan (*Escherichia coli*)—anthranilate synthetase, PR transferase, PRA isomerase, InGP synthetase, tryptophan synthetase". In: *Methods in Enzymology* 17 (1970). DOI: https://doi.org/10.1016/0076-6879(71)17215-1.

[38] V. Kriechbaumer *et al*. "Characterisation of the tryptophan synthase alpha subunit in maize". In: *BMC Plant Biology* 8 (2008). DOI: http://dx.doi.org/10.1186/1471-2229-8-44.

[39] R. Merkl. "Modelling the evolution of the archaeal tryptophan synthase". In: *BMC Evolutionary Biology* 7 (2007). DOI: https://doi.org/10.1186/1471-2148-7-59.

[40] G. Xie *et al*. "Significance of two distinct types of tryptophan synthase beta chain in Bacteria, Archaea and higher plants". In: *Genome Biology* 3 (2001). DOI: https://doi.org/10.1186/gb-2001-3-1-research0004.

[41] M. Ikeda. "Towards bacterial strains overproducing L-tryptophan and other aromatics by metabolic engineering". In: *Applied Microbiology and Biotechnology* 69 (2006). DOI: https://doi.org/10.1007/s00253-005-0252-y.

[42] J. Becker and C. Wittmann. "Bio-based production of chemicals, materials and fuels – *Corynebacterium glutamicum* as versatile cell factory". In: *Current Opinion in Biotechnology* 23 (2012). DOI: https://doi.org/10.1016/j.copbio.2011.11.012.

[43] H. Niu *et al*. "Metabolic engineering for improving L-tryptophan production in *Escherichia coli*". In: *Journal of Industrial Microbiology and Biotechnology* 46 (2018). DOI: https://doi.org/10.1007/s10295-018-2106-5.

[44] Z. Li *et al*. "Engineering *Escherichia coli* to improve tryptophan production via genetic manipulation of precursor and cofactor pathways". In: *Synthetic and Systems Biotechnology* 5 (2020). DOI: https://doi.org/10.1016/j.synbio.2020.06.009.

[45] M.G. López. Unpublished. 2022.

[46] T. Hoshino. "Violacein and related tryptophan metabolites produced by *Chromobacterium violaceum*: biosynthetic mechanism and pathway for construction of violacein core". In: *Applied Microbiology and Biotechnology* 91 (2011). DOI: https://doi.org/10.1007/s00253-011-3468-z.

[47] K. C. S. Queiroz *et al*. "Violacein Induces Death of Resistant Leukaemia Cells via Kinome Reprogramming, Endoplasmic Reticulum Stress and Golgi Apparatus Collapse". In: *PLOS ONE* 7 (2012). DOI: https://doi.org/10.1371/journal.pone.0045362.

[48] T. Mehta *et al*. "Violacein induces p44/42 mitogen-activated protein kinase-mediated solid tumor cell death and inhibits tumor cell migration". In: *Molecular Medicine Reports* 12 (2015). DOI: https://doi.org/10.3892/mmr.2015.3525.

[49] J. J. Füller *et al*. "Biosynthesis of Violacein, Structure and Function of l-Tryptophan Oxidase VioA from *Chromobacterium violaceum*". In: *Journal of Biological Chemistry* 291 (2016). DOI: https://dx.doi.org/10.1074%2Fjbc.M116.741561.

[50] N. Durán *et al*. "Advances in *Chromobacterium violaceum* and properties of violacein-Its main secondary metabolite: A review". In: *Biotechnology Advances* 34 (2016). DOI: https://doi.org/10.1016/j.biotechadv.2016.06.003.

[51] M.E. Lee *et al*. "Expression-level optimization of a multi-enzyme pathway in the absence of a high-throughput assay". In: *Nucleic Acids Research* 41 (2013). DOI: http://dx.doi.org/10.1093/nar/gkt809.

[52] K. Shinoda *et al*. "Biosynthesis of violacein: a genuine intermediate, protoviolaceinic acid, produced by VioABDE, and insight into VioC function". In: *Chemical Communications* 40 (2007). DOI: https://doi.org/10.1039/B705358D.

[53] J. Harrison and J. Ronczka. "An extraction of the violacein sequence from pJP101 for expression and analysis in pHSG398". In: *Journal of Innovation Impact* 6 (2013).

[54] G. Li and K.D. Young. "Indole production by the tryptophanase TnaA in *Escherichia coli* is determined by the amount of exogenous tryptophan". In: *Microbiology* 159 (2013). DOI: https://doi.org/10.1099/mic.0.064139-0.

[55] G. Li and K.D. Young. "A new suite of tnaA mutants suggests that *Escherichia coli* tryptophanase is regulated by intracellular sequestration and by occlusion of its active site". In: *BMC Microbiology* 15 (2015). DOI: https://doi.org/10.1186%2Fs12866-015-0346-3.

[56] A. Berstad *et al*. "Indole – the scent of a healthy 'inner soil'". In: *Microbial Ecology in Health and Disease* 26 (2015). DOI: https://doi.org/10.3402%2Fmehd.v26.27997.

[57] M.C. Deeley and C. Yanofsky. "Transcription initiation at the tryptophanase promoter of *Escherichia coli* K-12". In: *Journal of Bacteriology* 151 (1982). DOI: https://doi.org/10.1128/jb.151.2.942-951.1982.

[58] B.B. Williams *et al*. "Discovery and Characterization of Gut Microbiota Decarboxylases that Can Produce the Neurotransmitter Tryptamine". In: *Cell Host and Microbe* 16 (2014). DOI: https://doi.org/10.1016/j.chom.2014.09.001.

[59] Y. Bhattarai *et al*. "Gut Microbiota-Produced Tryptamine Activates an Epithelial G-Protein-Coupled Receptor to Increase Colonic Secretion". In: *Cell Host and Microbe* 23 (2018). DOI: https://doi.org/10.1016/j.chom.2018.05.004.

[60] R. Tittarelli *et al*. "Recreational Use, Analysis and Toxicity of Tryptamines". In: *Current Neuropharmacology* 13 (2015). DOI: https://doi.org/10.2174%2F1570159X13666141210222409.

[61] M.Z. Khan and W. Nawaz. "The emerging roles of human trace amines and human trace amine-associated receptors (hTAARs) in central nervous system". In: *Biomedicine and Pharmacotherapy* 83 (2016). DOI: https://doi.org/10.1016/j.biopha.2016.07.002.

[62] T. Watanabe and E.E. Snell. "Reversibility of the Tryptophanase Reaction: Synthesis of Tryptophan from Indole, Pyruvate, and Ammonia". In: *PNAS* 69 (1972). DOI: https://doi.org/10.1073%2Fpnas.69.5.1086.

[63] K. Amaratunga *et al*. "The methanol oxidation genes *mxaFJGIR(S)ACKLD* in *Methylobacterium extorquens*". In: *FEMS Microbiology Letters* 146 (1997). DOI: https://doi.org/10.1111/j.1574-6968.1997.tb10167.x.

[64] D. Hanahan. "Studies on Transformation of *Escherichia coli* with Plasmids". In: *Journal of Molecular Biology* 166 (1983). DOI: https://doi.org/10.1016/S0022-2836(83)80284-8.

[65] S. Ødegård. "Methanol-based production of heparosan and violacein in *Bacillus methanolicus* and *Methylobacterium extorquens*". MA thesis. Norwegian University of Science and Technology, May 2021.

[66] R. Higuchi *et al*. "A general method of in vitro preparation and specific mutagenesis of DNA fragments: study of protein and DNA interactions". In: *Nucleic Acids Research* 16 (1988). DOI: https://doi.org/10.1093%2Fnar%2F16.15.7351.

[67] A.V. Bryksin and I. Matsumura. "Overlap extension PCR cloning: a simple and reliable way to create recombinant plasmids". In: *BioTechniques* 48 (2018). DOI: https://doi.org/10.2144/000113418.

[68] D. G. Gibson *et al*. "Enzymatic assembly of DNA molecules up to several hundred kilobases". In: *Nature Methods* 6 (2009). DOI: https://doi.org/10.1038/nmeth.1318.

[69] Y. Tong *et al*. "Engineering oleaginous yeast *Yarrowia lipolytica* for violacein production: extraction, quantitative measurement and culture optimization." Unpublished. 2019. DOI: http://dx.doi.org/10.1101/687012.

[70] F. Pérez-García, L.F. Brito, and V.F. Wendisch. "Function of L-Pipecolic Acid as Compatible Solute in *Corynebacterium glutamicum* as Basis for Its Production Under Hyperosmolar Conditions". In: *Frontiers in Microbiology* 10 (2019). DOI: https://doi.org/10.3389%2Ffmicb.2019.00340.

[71] Y. Zhou *et al*. "Enhanced Production of Crude Violacein from Glucose in *Escherichia coli* by Overexpression of Rate-Limiting Key Enzyme(S) Involved in Violacein Biosynthesis". In: *Applied Biochemistry and Biotechnology* 186 (2018). DOI: https://doi.org/10.1007/s12010-018-2787-2.

[72] A.L. Rodrigues *et al*. "Systems metabolic engineering of *Escherichia coli* for production of the antitumor drugs violacein and deoxyviolacein". In: *Metabolic Engineering* 20 (2013). DOI: https://doi.org/10.1016/j.ymben.2013.08.004.

[73] C.J. Balibar and C.T. Walsh. "In Vitro Biosynthesis of Violacein from l-Tryptophan by the Enzymes VioA-E from *Chromobacterium violaceum*". In: *Biochemistry* 45 (2006). DOI: https://doi.org/10.1021/bi061998z.

[74] H. Sun *et al*. "Engineering *Corynebacterium glutamicum* for violacein hyper production". In: *Microbial Cell Factories* 15 (2016). DOI: https://doi.org/10.1186/s12934-016-0545-0.

[75] W.-T. Chan *et al*. "A comparison and optimization of methods and factors affecting the transformation of *Escherichia coli*". In: *Bioscience Reports* 33 (2013). DOI: https://doi.org/10.1042%2FBSR20130098.

[76] G. Nagamani *et al*. "A novel approach for increasing transformation efficiency in *E. coli* DH5α cells using silver nanoparticles". In: *3 Biotech* 9 (2019). DOI: https://doi.org/10.1007%2Fs13205-019-1640-9.

[77] H.-A. Choi *et al*. "A simple bacterial transformation method using magnesium- and calcium-aminoclays". In: *Journal of Microbiological Methods* 95 (2013). DOI: https://doi.org/10.1016/j.mimet.2013.07.018.

[78] L. F. Brito *et al*. "Magnesium aminoclay-based transformation of *Paenibacillus riograndensis* and *Paenibacillus polymyxa* and development of tools for gene expression". In: *Applied Microbiology and Biotechnology* 101 (2017). DOI: https://doi.org/10.1007/s00253-016-7999-1.

[79] G.P. Mendes *et al*. "Magnesium aminoclays as plasmid delivery agents for non-competent *Escherichia coli* JM109 transformation". In: *Applied Clay Science* 204 (2021). DOI: https://doi.org/10.1016/j.clay.2021.106010.

[80] Y. Zhang *et al*. "Direct RBS Engineering of the biosynthetic gene cluster for efficient productivity of violaceins in *E. coli*". In: *Microbial Cell Factories* 20 (2021). DOI: https://doi.org/10.1186/s12934-021-01518-1.

[81] L.A. Moran et al. *Principles of Biochemistry*. 5th ed. Pearson, 2014.

[82] F. Belinky *et al*. "Selection on start codons in prokaryotes and potential compensatory nucleotide substitutions". In: *Scientific Reports* 7 (2017). DOI: https://doi.org/10.1038/s41598-017-12619-6.

[83] T.R. Garbe *et al*. "Indole-inducible proteins in bacteria suggest membrane and oxidant toxicity". In: *Archives of Microbiology* 173 (2000). DOI: https://doi.org/10.1007/s002030050012.

[84] J. Liu and D.K. Summers. "Indole at low concentration helps exponentially growing *Escherichia coli* survive at high temperature". In: *PLOS ONE* 12 (2017). DOI: http://dx.doi.org/10.1371/journal.pone.0188853.

[85] T. Brautaset *et al*. "Role of the *Bacillus methanolicus* Citrate Synthase II Gene, *citY*, in Regulating the Secretion of Glutamine in L-Lysine-Secreting Mutants". In: *Applied and Environmental Microbiology* 69 (2020). DOI: https://doi.org/10.1128/AEM.69.7.3986-3995.2003.

APPENDIX A
SUPPLEMENTARY MATERIAL FOR MOLECULAR DNA WORK

Table A.1: List of DNA primers used for DNA amplification by PCR, divided according to constructs. T_A: annealing temperature. Uppercase letters indicate overhang regions for respective plasmids.

Primer name	Description	T_A (°C)	Sequence
mgl135	Forward primer for DNA amplification of *vioA*	67	AACTTGTTCACTTAAGGGGGAAATGACAAatgaagcattcttccgatatctg cattgtcggcgccgg
mgl136	Reverse primer for DNA amplification of *vioA*	67	cgactatgattgctcttttcatATGGCACGTATTAATGCGtcacgcggcgatgcgctgc agcagcag
mgl137	Forward primer for DNA amplification of *vioC*	62	gctgcagcgcatcgccgcgtgaCGCATTAATACGTGCCATatgaaaagagcaatcat agtcggaggcggg
mgl138	Reverse primer for DNA amplification of *vioC*	62	cgccgatgaccagaatcttcatATGGCACGTATTAATGCGtcagttgaccctccctatc ttgtaccaaac
mgl139	Forward primer for DNA amplification of *vioD*	67	caagatagggagggtcaactgaCGCATTAATACGTGCCATatgaagattctggtcatc ggcgcggggccg
mgl140	Reverse primer for DNA amplification of *vioD*	67	TTGTAAAACGACGGCCAGTGAATTCGAGCTtcagcgttgcagcgcgtagc gcaggttctg
mgl141	Forward primer for DNA amplification of *vioABC*	63	AACTTGTTCACTTAAGGGGGAAATGACAAatgaagcattcttccgatatctg cattgtc
mgl142	Reverse primer for DNA amplification of *vioABC*	63	gcggcggttcccggttttccatATGGCACGTATTAATGCGtcagttgaccctccctatct tgtaccaaac
mgl143	Forward primer for DNA amplification of *vioE*	63	caagatagggagggtcaactgaCGCATTAATACGTGCCATatggaaaaccgggaac cgccgctgctgccg
mgl014	Reverse primer for DNA amplification of *vioE*	62	ACGGCCAGTGAATTCGAGCTctagcgcttggcggcgaaga
mgl155	Forward primer for DNA amplification of *vioB*	64	CATGTGAGACGAGCTCGGTACCCGGGGATCatgagcattctggattttcca cgcatccat
mgl145	Reverse primer for DNA amplification of *vioB*	64	gcggcggttcccggttttccatATGGCACGTATTAATGCGtcaggcctctctagaaag ctttccacaagc
mgl146	Forward primer for DNA amplification of *vioE*	68	aaagctttctagagaggcctgaCGCATTAATACGTGCCATatggaaaaccgggaacc gccgctgctgccg
mgl147	Reverse primer for DNA amplification of *vioE*	68	TGCATGCCTGCAGGTCGACTCTAGAGGATCctagcgcttggcggcgaag acggcgtcggg
mgl156	Forward primer for DNA amplification of *vioD*	67	CATGTGAGACGAGCTCGGTACCCGGGGATCatgaagattctggtcatcgg cgcggggccg
mgl149	Reverse primer for DNA amplification of *vioD*	67	TGCATGCCTGCAGGTCGACTCTAGAGGATCtcagcgttgcagcgcgtagc gcaggttctg
mgl157	Forward primer for DNA amplification of *vioE*	69	CATGTGAGACGAGCTCGGTACCCGGGGATCatggaaaaccgggaaccg ccgctgctgccg
mgl151	Reverse primer for DNA amplification of *vioE*	68	TGCATGCCTGCAGGTCGACTCTAGAGGATCctagcgcttggcggcgaag acggcgtcggg
mgl164	Forward primer for DNA amplification of PP_2552	65	AACTTGTTCACTTAAGGGGGAAATGACAAgtgacccccgaacaattccgc cagtacggc
mgl165	Reverse primer for DNA amplification of PP_2552	65	GCTCTAGACGACGGCCAGTGAATTCGAGCTtcagcccttgatcacgtcctg cagacgtgc
mgl170	Forward primer for DNA amplification of *tnaA*	58	AACTTGTTCACTTAAGGGGGAAATGACAAatggaaaactttaaacatctcc ctgaaccg
mgl171	Reverse primer for DNA amplification of *tnaA*	58	GCTCTAGACGACGGCCAGTGAATTCGAGCTttaaacttctttaagttttgcgg tgaagtg

Table A.2: List of DNA primers used for OE-PCR. T_A: annealing temperature. Uppercase letters indicate overhang regions for respective plasmids.

Primer name	Description	T_A (°C)	Sequence
mgl015	Forward primer for DNA amplification of *vioA* with *B. methanolicus* RBS	62	CTTAAGGGGGAAATGGGATCatgaagcattcttc cgatatctgcattgtcggcgccggcatcagc
mgl016	Reverse primer for DNA amplification of *vioA* with *B. methanolicus* RBS	62	ggaaaatccagaatgctcatctgaagggcctcctttctcacgcggc gatgcgctgca
mgl017	Forward primer for DNA amplification of *vioB* with *B. methanolicus* RBS	67	tgcagcgcatcgccgcgtgagaaaggaggcccttcagatgagca ttctggattttcc
mgl018	Reverse primer for DNA amplification of *vioB* with *B. methanolicus* RBS	67	actatgattgctcttttcatctgaagggcctcctttctcaggcctctct agaaagct
mgl019	Forward primer for DNA amplification of *vioC* with *B. methanolicus* RBS	59	agctttctagagaggcctgagaaaggaggcccttcagatgaaaag agcaatcatagtcg
mgl020	Reverse primer for DNA amplification of *vioC* with *B. methanolicus* RBS	59	ccgatgaccagaatcttcatctgaagggcctcctttctcagttgacc ctccctatct
mgl009	Forward primer for DNA amplification of *vioD* with *B. methanolicus* RBS	62	cgttggtcggcaagtcctgggaaaggaggcccttcagatgaaaat cctcgtcatcggcgc
mgl010	Reverse primer for DNA amplification of *vioD* with *B. methanolicus* RBS	62	ggggtggcgtgcggtggcatctgaagggcctcctttcttagcggc cgagggcgtagc
mgl023	Forward primer for DNA amplification of *vioE* with *B. methanolicus* RBS	62	gctacgcgctgcaacgctgagaaaggaggcccttcagatggaaa accgggaaccgcc
mgl024	Reverse primer for DNA amplification of *vioE* with *B. methanolicus* RBS	62	CGACGGCCAGTGAATTCGAGCTctagcgcttg gcggcgaagacggcg

Table A.3: List of DNA primers used for sequencing, forward and reverse primers are also used for cPCR. T_A: annealing temperature. Uppercase letters indicate overhang regions for respective plasmids.

Primer name	Description	T_A (°C)	Sequence
mgl121	Forward sequencing primer for pBV2xp/pUB110Sxp	51	GCTTGATCTGCAATTTGAAT
mgl106	Reverse sequencing primer for pBV2xp	51	CAAAACGCATACCATTTTG
mgl112	Forward sequencing primer for pNW33Nmp	50	GCGTCAAAATCACTTTTCCTTTGG
mgl154	Reverse sequencing primer for pNW33Nmp	50	CTAATGTCACTAGGGCTCGC
mgl169	Reverse sequencing primer for pUB110Sxp	54	CCTTTGCTGAGGTGGCAGAG
mgl067	Sequencing primers for *vioABCDE*		ccagggccatgacagcgcgg
mgl068			cggctacctggagcagatcc
mgl069			cgcggccggcaacaaccatttc
mgl070			ggccggccggctgctgcgtc
mgl071			cccgctgcgggtgctgccgg
mgl072			gatggcgctgggcgagccgttc
mgl073			gcacttcgcggtcaagccgc
mgl074			ggcgttttccgtcggcggcc
mgl075			caacgacctgatcaacgtcc
mgl076			ggccaatccgctgtcctacc
mgl077			gagccacgaccgctgccacg
mgl078			gcagaaggtggcctatggcc
mgl167	Sequencing primers for PP_2552		gagcgaactggaagaaaccacc
mgl168			ggtcaacgcgcacaaatggc
mgl172	Sequencing primers for *tnaA*		gcagagcaaatctatattccgg
mgl173			ccgagtgcagaaccctttgcg

APPENDIX B
GROWTH MEDIA COMPOSITION

Table B.1: Composition of growth media and other solutions used in this study

Medium name	Component	Concentration (g/L)	Ref.
Super Optimal Broth (SOB)	Hanahan's Broth	28	[64]
	MeOH	1% v/v	
	Agar	15	
Lysogeny Broth (LB)	Yeast extract	5	
	Tryptone	10	
	NaCl	10	
	Agar	15	
MVcM	See reference for composition		[85]
MVcMY	See reference for composition		[85]
Electroporation Buffer (EPB)	HEPES	0.06	
	PEG_{8000}	62.5	

APPENDIX C
GROWTH DATA

Table C.1: OD_{600} measurements of *B. methanolicus* MGA3 harbouring pBV2xp-*vioABCDE* and empty control vector pBV2xp cultivated in MVcM medium, in triplicates. Cultures cultivated at 50°C and 200 RPM for 12h, then at 30°C and 200 RPM until 48h. Induction of all cultures after 2h, HPLC samples taken after 2, 4, 8, 12, 24 and 48h.

	t (h)	0	2	4	6	8	11	12	24	48
	1	0.13	0.22	0.42	1.40	1.60	7.00	6.00	4.60	1.80
pBV	2	0.12	0.25	0.60	1.70	3.20	6.50	5.20	2.80	0.60
	3	0.13	0.26	0.55	1.70	2.90	5.90	4.90	3.10	0.60
	1	0.12	0.24	0.50	1.00	2.60	5.00	6.30	5.10	2.10
pVio	2	0.12	0.26	0.56	1.80	3.00	6.00	5.90	1.90	0.60
	3	0.12	0.23	0.51	1.80	3.00	6.00	5.40	2.60	0.80

pBV: *B. methanolicus* MGA3(pBV2xp)
pVio: *B. methanolicus* MGA3(pBV2xp-*vioABCDE*)

Table C.2: OD_{600} measurements of *B. methanolicus* MGA3 harbouring (pBV2xp-*vioACD*)(pNW33Nmp-*vioBE*) and empty control vectors pBV2xp and pNW33Nmp cultivated in MVcM medium, in triplicates. Cultures cultivated at 50°C and 200 RPM for 12h, then at 37°C and 200 RPM until 48h. Induction of all cultures after 2h, HPLC samples taken after 4, 8, 12, 24 and 48h.

	t (h)	0	2	4	6	8	10	12	14	15	24	48
	1	0.10	0.16	0.36	0.73	2.30	5.20	5.40	3.70	3.00	0.50	0.80
pBV	2	0.03	0.03	0.05	0.06	0.12	0.21	0.35	0.79	1.10	0.90	0.90
	3	0.02	0.03	0.02	0.02	0.02	0.02	0.02	0.02	0.02	0.02	0.02
	1	0.27	0.44	1.16	2.20	5.70	6.20	5.40	3.00	2.40	0.80	0.80
pNW	2	0.27	0.48	1.16	2.70	6.20	8.50	5.30	4.80	3.90	1.70	1.20
	3	0.29	0.42	1.14	2.30	5.80	6.80	5.20	2.30	1.80	1.20	0.56
	1	0.34	0.39	0.68	1.30	3.60	6.70	5.40	3.90	3.20	1.30	0.66
pACDBE	2	0.28	0.31	0.54	1.10	2.90	6.40	5.40	3.90	3.30	1.30	0.58
	3	0.28	0.34	0.64	1.30	3.90	6.80	4.50	3.40	2.90	1.20	0.58

pBV: *B. methanolicus* MGA3(pBV2xp)
pNW: *B. methanolicus* MGA3(pNW33Nmp)
pACDBE: *B. methanolicus* MGA3(pBV2xp-*vioACD*)(pNW33Nmp-*vioBE*)

Table C.3: OD_{600} measurements of *B. methanolicus* MGA3 harbouring pUB110Sxp-*tnaA* and empty control vector pUB110Sxp cultivated in MVcM medium, in triplicates. pUB cultivated at 50°C and 200 RPM for 12h, then at 37°C and 200 RPM until 48h, pTnaA cultivated at 50°C for 48h. Induction of all cultures after 2h, HPLC samples taken after 4, 8, 12, 24 and 48h.

	t (h)	0	2	4	6	8	10	12	14	15	24	48
	1	0.30	0.47	0.87	2.10	4.30	7.60	5.60	4.20	3.70	0.80	0.52
pUB	2	0.24	0.40	0.85	1.90	4.50	7.00	4.30	4.50	3.10	1.30	0.33
	3	0.28	0.42	0.96	1.90	4.80	7.60	5.40	4.10	3.70	0.80	0.71
	1	0.28	0.44	0.77	1.20	2.00	3.70	4.30	4.70	4.60	2.40	3.48
pTnaA	2	0.28	0.44	0.81	1.30	2.50	3.80	4.60	3.90	3.40	2.00	4.56
	3	0.27	0.49	0.78	1.20	2.40	3.60	4.90	4.10	3.80	2.40	3.10

pUB: *B. methanolicus* MGA3(pUB110Sxp)
pTnaA: *B. methanolicus* MGA3(pTH1mp-Trp3)(pUB110Sxp-*tnaA*)

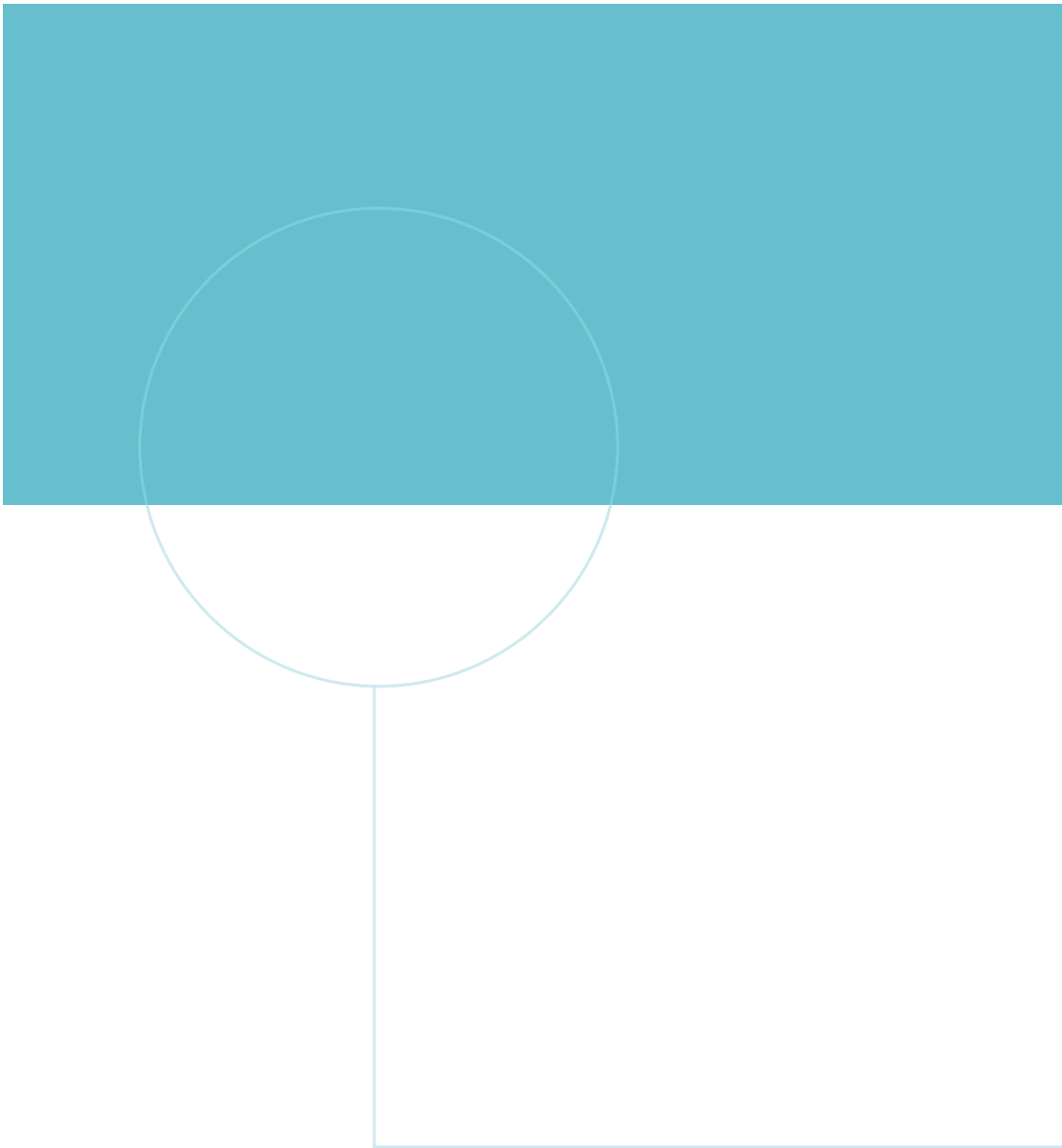

NTNU

Norwegian University of
Science and Technology